

**MAXIMIZING siRNA DELIVERY EFFICIENCY**  
**WITH PHOTO-RESPONSIVE**  
**POLYMER NANOCARRIERS**

by

Victoria Grace Muir

A thesis submitted to the Faculty of the University of Delaware in partial fulfillment of the requirements for the degree of Honors Bachelor's of Chemical Engineering with Distinction

Spring 2018

© 2018 Muir  
All Rights Reserved

**MAXIMIZING siRNA DELIVERY EFFICIENCY  
WITH PHOTO-RESPONSIVE  
POLYMER NANOCARRIERS**

by

Victoria Grace Muir

Approved: \_\_\_\_\_  
Millicent O. Sullivan, Ph.D.  
Professor in charge of thesis on behalf of the Advisory Committee

Approved: \_\_\_\_\_  
Thomas H. Epps, III, Ph.D.  
Committee member from the Department of Chemical & Biomolecular  
Engineering

Approved: \_\_\_\_\_  
Jason Gleghorn, Ph.D.  
Committee member from the Board of Senior Thesis Readers

Approved: \_\_\_\_\_  
Paul Laux, Ph.D.  
Director, University Honors Program

## ACKNOWLEDGMENTS

I would like to thank my researcher advisors and mentors, Professor Millie Sullivan and Professor Thomas H. Epps, III. Professor Epps provided me with an opportunity to conduct research in polymer thin films while I was in my sophomore year of high school at the Charter School of Wilmington through the American Chemical Society (ACS) Project SEED. As a high school student in the Epps Group, I gained an interest in the field of chemical engineering research that completely changed my career prospects and started me on the road to becoming an engineering professor. For the past six years, Professor Epps has been nothing short of an incredible resource and inspiration for my future career. When I started as a freshman at University of Delaware (UD), I wanted to explore applications of polymers in medicine, and Professor Epps granted me the opportunity to be co-advised with Professor Sullivan on the photo-responsive siRNA delivery project. Through working with Professor Sullivan, I found my research niche of biomaterials, which is the field I hope to pursue in my career as a professor. Professor Sullivan has been an outstanding role model for strong females in engineering and academia. I will forever be grateful to Professor Epps and Professor Sullivan for their guidance and mentorship in my undergraduate career.

I also want to thank two very special graduate students, Jill Emerson and Chad Greco. When I started as a high school student in the Epps Group, Jill was my graduate student mentor. Being that I had only taken one introductory high school chemistry class when joining the lab, there was quite a learning curve to understand

polymer thin films and conduct research experiments. Jill was always a bright and friendly face, and she was wonderful in answering my many, many questions. Jill became not only my mentor, but also my friend, and I am very grateful for her mentorship in starting my research journey. I would also like to thank Chad Greco, my graduate student mentor for the biomaterials work in my thesis. Chad got the pleasure of having not one, but two undergraduate students follow him around like ducklings all day asking questions about polyplexes. Chad was always more than willing to help, and he also was a great example of having a good work-life balance in graduate school. I owe so much to Jill and Chad for being amazing mentors.

There were many other people in the Epps and Sullivan Groups who have been helpful in putting my thesis together. Special thanks to Jason Andrechak for putting up with all my questions and overall being a “gr8” person. I would also like to thank Vi and Esther for being my polyplex resources during this past year after Chad and Jason have graduated. Additionally, thanks to Lucas, Colleen, and Rachel for helping me set up new experiments for my thesis work.

Outside of the Epps and Sullivan groups, there are so many people at UD that I am grateful for. All the UD Honors Program staff have been so supportive in helping me apply for scholarships and fellowships. I especially would like to thank Kristin Benninghoff for spending hours with me combing through grad school and fellowship applications while trying not to get distracted by the latest Zumba news in Delaware. I also want to thank Professor Ismat Shah for taking me on study abroad adventures twice and giving me the travel bug. Additionally, thanks to everyone in the department that has helped along the way while I have been a leader of the AIChE student chapter, especially Megan Argoe and Professor Josh Enszer.

Lastly, I want to thank my amazing friends and family for supporting me through undergrad and letting me tell them about polyplexes. Special thank you to Rob for spending many date nights helping me set up Excel sheets for nanocarrier formulations and make figures for presentations. And, most importantly, thank you to my mom, Julia, for being the absolute best mom a girl could ever ask for.

## TABLE OF CONTENTS

LIST OF FIGURES .....	7
ABSTRACT .....	10
1 INTRODUCTION AND MOTIVATION.....	11
1.1 RNA interference (RNAi) .....	11
1.2 siRNA delivery methods .....	11
1.2.1 Viral vectors .....	12
1.2.2 Non-viral vectors .....	12
1.3 Cationic polymer nanocarriers for siRNA.....	13
1.4 Photo-responsive polymer for siRNA delivery .....	14
1.5 Thesis summary.....	15
2 MATERIALS AND METHODS .....	17
2.1 Materials .....	17
2.2 Methods .....	18
2.2.1 Single-layer polyplex nanocarrier formulation .....	18
2.2.2 Multi-layer polyplex nanocarrier formulation.....	19
2.2.3 Ethidium bromide gel electrophoresis.....	19
2.2.4 Photo-responsive siRNA release .....	19
2.2.5 Polyplex size determination .....	20
2.2.5.1 Fluorescence correlation microscopy (FCS) .....	20
2.2.5.2 Dynamic light scattering (DLS) .....	20
2.2.6 Determining charge with zeta potential.....	21
2.2.7 Cell culture and transfection.....	21
2.2.8 Cellular uptake.....	22
2.2.9 Gene silencing analysis .....	22
2.2.10 mRNA silencing .....	24
2.2.11 Kinetic modeling .....	24
3 COMBINING MIXED POLYMER NANOCARRIERS WITH SIMPLE KINETIC MODELING TO TUNE siRNA DOSE RESPONSE .....	26
3.1 Background and motivation .....	26
3.1.1 Mixed polyplexes .....	26
3.1.2 Kinetic modeling and dosing schedule.....	26

3.2	Research Aims 1 and 2 – Mixed polyplexes combined with kinetic modeling.....	27
3.3	Results and discussion.....	28
3.3.1	Mixed polyplex siRNA encapsulation.....	28
3.3.2	Gene silencing.....	30
3.3.3	Light-induced siRNA release.....	32
3.3.4	Cellular uptake.....	33
3.3.5	Polyplex size and charge.....	35
3.3.6	Kinetic modeling.....	37
3.3.6.1	Single polyplex dose.....	37
3.3.6.2	Repeated polyplex dose and predictive dosing schedule.....	40
3.4	Conclusions.....	42
4	LAYERED NANOCARRIERS FOR SEQUENTIAL RELEASE OF MULTIPLE siRNAs.....	45
4.1	Background and motivation.....	45
4.1.1	Controlled delivery of multiple doses of siRNA.....	45
4.1.2	Research aim 3 - layered, photo-responsive nanocarriers for delivery of multiple siRNAs.....	46
4.2	Results and discussion.....	47
4.2.1	Design 1 – Block copolymer inner layer.....	47
4.2.2	Simple formulation approach.....	48
4.2.2.1	Revised formulation approach – centrifugation between layers.....	51
4.2.3	Design 2 – homopolymer inner layer.....	53
4.3	Conclusions.....	55
5	CONCLUSIONS.....	58
6	FUTURE WORK.....	59
6.1	Co-delivery systems.....	59
6.2	Photo-responsive thin film for siRNA delivery.....	60

REFERENCES .....	61
APPENDIX: TEXT AND FIGURE REPRINT PERMISSIONS .....	65

## LIST OF FIGURES

- Figure 1-1. Photo-responsive polyplexes. A) Diblock copolymer mPEG-*b*-P(APNBMA)<sub>n</sub> structure. B) Photo-responsive polyplex assembly. .... 15
- Figure 3-1. Mixed polyplex structure. .... 28
- Figure 3-2. Gel electrophoresis assay of mPEG-*b*-P(APNBMA)<sub>n</sub>/siRNA polyplexes. A) Gel electrophoresis of polyplexes formed at varying total N:P ratios. B) Quantification of gel electrophoresis images based on ImageJ analysis of siRNA bands. Figure is reprinted from Greco and Muir et. al. with permissions from Elsevier.<sup>18</sup> ..... 29
- Figure 3-3. GAPDH protein expression levels as a function of molar composition of mPEG-*b*-P(APNBMA)<sub>7.9</sub> / mPEG-*b*-P(APNBMA)<sub>23.6</sub>.<sup>18</sup> Cells were treated with siRNA polyplexes and subsequently exposed to UV light for 10 min and lysed for western blot analysis 48 h post-transfection. Data represent the GAPDH protein expression levels relative to the levels of the loading control β-actin, normalized to the native protein levels in controls with no siRNA treatment. Results are shown as the mean ± standard deviation of data obtained from three independent experiments. Statistical significance compared to the 50/50 formulation is marked with an “\*”. Figure is reprinted from Greco and Muir et. al. with permissions from Elsevier.<sup>18</sup> ..... 31
- Figure 3-4. Light-mediated release of siRNA from mPEG-*b*-P(APNBMA)<sub>n</sub>/siRNA polyplexes.<sup>18</sup> Polyplexes were formed at an N:P of 4 and exposed to SDS solutions at an S:P of 2.5 before being irradiated with UV light for 10 min. The amount of free siRNA was quantified *via* ImageJ analysis of gel electrophoresis experiments. Figure is reprinted from Greco and Muir et. al. with permissions from Elsevier.<sup>18</sup> ..... 33
- Figure 3-5. Cellular uptake of mPEG-*b*-P(APNBMA)<sub>n</sub>/siRNA polyplexes.<sup>18</sup> Fluorescently tagged siRNA was incorporated into polyplexes and delivered to cells for flow cytometry analysis. The mean fluorescence intensity per cell was normalized to the 0/100 polyplexes. Results are shown as the mean ± standard deviation of data obtained from three independent samples. Figure is reprinted from Greco and Muir et. al. with permissions from Elsevier.<sup>18</sup> ..... 34

Figure 3-6. Average zeta potentials (light blue, associated with primary y-axis) and diameters (pink, associated with secondary y-axis) of polyplexes with varying compositions.<sup>18</sup> Polyplexes were formed at a total N:P of 4, with different polymer compositions of mPEG-*b*-P(APNBMA)<sub>7.9</sub>/mPEG-*b*-P(APNBMA)<sub>23.6</sub>, on a molar basis of cationic amine groups. Results are shown as the mean ± standard deviation of data obtained from three independent measurements. Figure is reprinted from Greco and Muir et. al. with permissions from Elsevier.<sup>18</sup> ..... 36

Figure 3-7. Mass action kinetic models predict the dynamic nature of the GAPDH silencing process with a single dose (A) of siRNA.<sup>18</sup> Initial protein and mRNA concentrations were normalized to 100 to simulate steady-state conditions. After application of UV light, 100 normalized units of siRNA were introduced. The UV light was applied 3.5 h after each transfection. B) Cells were lysed at 48 h following either a single dose of siRNA. GAPDH mRNA and protein expression levels were determined through qPCR and western blot experiments, respectively. Model predictions of mRNA (green) and protein (orange) expression levels at the end points of 48 h are presented as solid bars; experimental values are presented as diagonal striped bars. Experimental values are shown as the mean ± standard deviation of data obtained from three independent samples. Figure is reprinted from Greco and Muir et. al. with permissions from Elsevier.<sup>18</sup> ..... 39

Figure 3-8. Mass action kinetic models predict the dynamic nature of the GAPDH silencing process with a double dose of siRNA.<sup>18</sup> Initial protein and mRNA concentrations were normalized to 100 to simulate state-state conditions. After application of UV light, 100 normalized units of siRNA were introduced. The UV light was applied 3.5 h after each transfection. B) Cells were lysed at 75 h following either a double dose of siRNA. GAPDH mRNA and protein expression levels were determined through qPCR and western blot experiments, respectively. Model predictions of mRNA (green) and protein (orange) expression levels at the end points of 75 h are presented as solid bars; experimental values are presented as diagonal striped bars. Experimental values are shown as the mean ± standard deviation of data obtained from three independent samples. Figure is reprinted from Greco and Muir et. al. with permissions from Elsevier.<sup>18</sup> ..... 42

Figure 4-1. Schematic representation of the layered polyplex formulations explored in this work. Red indicates siRNA, blue indicates a photo-responsive polymer, and green indicates PEG block. The lighter blue photo-responsive polymer inner layer is varied in the experiments herein. ....	47
Figure 4-2. Proposed formulation of creating layered nanocarriers in Design 1 using block copolymers for each polymer layer. ....	48
Figure 4-3. Initial proposed layering procedure using Design 1. A) Size measurements of nanocarriers. B) Zeta potential measurements of nanocarriers. Error bars indicate $\pm 1$ standard deviation from 3 experimental replicates. ....	50
Figure 4-4. Procedural centrifugation purification steps for layered polyplex formulation using Design 1. ....	52
Figure 4-5. Revised layering formulation approach with homopolymer inner layer and purification <i>via</i> centrifugation between each layer addition. ....	54
Figure 4-6. Revised layering procedure using Design 2 and homopolymer inner layer. A) Size measurements of nanocarriers. B) Zeta potential measurements of nanocarriers. Error bars indicate $\pm 1$ standard deviation from 3 experimental replicates. ....	55
Figure 4-7. Representative microscopy images of proposed experiment to demonstrate successful control over releasing each layer of siRNA. A) Cells express both GFP and RFP. B) After delivering layered polyplexes, over increasing exposure to light stimulus, GFP will be silencing first, followed by RFP. ....	57

## ABSTRACT

In that last few decades, there has been a great interest in developing small interfering RNA (siRNA) therapeutics and research tools. There are many challenges that limit success of siRNA therapeutics, including control over siRNA release, lack of predictability, and the need for multiple doses of siRNA for sustained treatment. In this thesis, those challenges are addressed through the formulation of photo-responsive polyplexes for siRNA delivery. Mixed polyplexes were created by mixing two photo-responsive block copolymers to optimize polyplex properties, including size and zeta potential. It was found that a 50/50 mixture of the two polymers was able to achieve 70% protein knockdown of glyceraldehyde 3-phosphate dehydrogenase (GAPDH), which is suggested to be the maximum amount of GAPDH silencing possible in a single dose of siRNA. Furthermore, a simple kinetic model was employed to predict siRNA, messenger RNA (mRNA), and protein concentrations in the cell over time and develop a dosing schedule. These predictions enabled the application of a second dose of siRNA to suppress gene expression over three days, leading to a further 50% reduction in protein levels compared to a single dose. Polyplexes remained dormant in cells until exposed to light, demonstrating the complete control over siRNA activity as well as the stability of the nanocarriers. Additionally, a layered, photo-responsive system was developed to obtain controlled release over multiple doses of siRNA from a single particle. Thus, this work demonstrates that simple kinetic modeling and straightforward biomaterials design can be used to suppress gene expression maximally for an siRNA delivery system.

## Chapter 1

### INTRODUCTION AND MOTIVATION

#### 1.1 RNA interference (RNAi)

The RNA interference pathway (RNAi) is a powerful method of gene regulation that occurs in eukaryotic cells.<sup>1</sup> In the RNAi pathway, short double-stranded pieces of RNA, called small interfering RNA (siRNA), activate a gene silencing protein complex called the RNA-induced silencing complex (RISC). Once activated, RISC cleaves target strands of messenger RNA (mRNA) and post-transcriptionally down-regulates protein expression. Harnessing the power to silence proteins temporarily is of great interest for use as a research tool or as a therapeutic approach. Billions of dollars have been spent on siRNA research since the discovery of siRNA by Fire and Mello in 1998.<sup>2</sup> RNAi-based medical treatments are being explored to address diseases, including cancers and cardiovascular issues.<sup>3</sup>

#### 1.2 siRNA delivery methods

There are multiple challenges to utilizing siRNA as a therapeutic. Molecules of siRNA are negatively charged and cannot pass across cell membranes on their own. Additionally, 'naked' siRNAs are subject to degradation by ribonuclease (RNase) enzymes throughout the body.<sup>4</sup> Furthermore, custom siRNA synthesis is an expensive and time-consuming process. Predictability of siRNA release also is a concern, since many applications require precise control over gene silencing kinetics. To address some of these challenges, siRNA can be packaged into a delivery vehicle for protection from nuclease degradation and control over siRNA release. Delivery vehicles are often categorized as either viral vectors or non-viral vectors.

### **1.2.1 Viral vectors**

Viruses have evolved over millions of years to be efficient delivery vehicles for nucleic acids. Once bound to the cell membrane, virus particles can inject nucleic acid cargoes directly into the cytoplasm or orchestrate endocytic uptake and subcellular transport, which is beneficial since the RISC forms in the cytoplasm.<sup>5,6</sup> However, there are many concerns with using viral vectors as siRNA delivery vehicles, including patient inflammatory response, immunogenicity, and oncogenicity of virus particles.<sup>7</sup> At the University of Pennsylvania, a patient in a viral-vector gene therapy clinical trial for delivering deoxyribonucleic acid (DNA) as a treatment for liver disease passed away from side effects of the viral vector treatment.<sup>8</sup> The toxicity concerns over use of viral vectors limit their potential for clinical translation of siRNA therapeutics. Additionally, viral vectors are costly and relatively small, so there is a limit to how much cargo can be loaded. Furthermore, viral vectors are not particularly effective for siRNA delivery and are better suited for delivering DNA or mRNA.

### **1.2.2 Non-viral vectors**

Due to the toxicity and manufacturing concerns of viral vectors, non-viral vectors are the promising delivery vehicles for nucleic acids.<sup>5</sup> Non-viral vectors can be customized easily for specific applications, and stimuli-responsive elements can be incorporated to add additional levels of control over siRNA delivery to meet the need for predictability and control in gene silencing.<sup>9,10</sup> Two main challenges to non-viral siRNA delivery are the low delivery efficiency of siRNA and the issue of gaining complete control over siRNA release.

### 1.3 Cationic polymer nanocarriers for siRNA

Cationic polymer nanocarriers in particular are promising delivery vehicles for siRNA due to their tunability and biocompatibility.<sup>11</sup> Cationic polymers self-assemble *via* electrostatic interactions with siRNAs to form nanocarrier structures called polyplexes. The polymers form a protective structure around the negatively charged siRNA core. Ideal polymer nanocarriers will efficiently encapsulate siRNA to protect it from degradation as well as incorporate a mechanism for endosomal escape and intracellular delivery.<sup>12</sup>

There are many challenges to developing effective polyplex delivery systems, including obtaining proper size, surface charge, biocompatibility, and unpackaging kinetics and mechanisms.<sup>11</sup> Polyplex systems must balance the seemingly contradictory demands of sufficient siRNA binding and encapsulation with siRNA release capabilities.<sup>13</sup> Furthermore, polyplexes must be small enough to be internalized by cells, but also have enough positive surface charge to promote internalization, without having too high of a cationic charge density to become cytotoxic.<sup>13</sup> Balancing all these requirements creates challenges to designing polymer nanocarriers that are efficient vehicles for siRNA delivery. To address some of these challenges, stimuli-responsive elements can be incorporated into polyplex structures.

Stimuli-responsive elements often are incorporated into polymer nanocarriers for control of siRNA release, which can increase delivery efficiency and reduce off-target effects.<sup>10</sup> Polyplexes can be designed to release siRNA upon exposure to internal stimuli, such as pH or enzymes, or external stimuli, such as temperature and light. Among these stimuli, light-responsive nanoparticles are attractive due to their ease of spatiotemporally controlled release, as well as their precision and flexibility.<sup>14</sup> Using light as a stimulus enables precise on/off control over siRNA release so that

gene silencing can be directed accurately. In practice, light-responsive polyplexes would be beneficial to deliver siRNA in topical applications, such as skin cancers, as well as some surgical applications, such as wound healing, since light can penetrate these tissues.

#### **1.4 Photo-responsive polymer for siRNA delivery**

Previously, the Epps and Sullivan groups at the University of Delaware developed a photo-responsive polymer for siRNA delivery.<sup>15-17</sup> The novel mPEG-*b*-poly(5-(3-(amino)propoxy)-2-nitrobenzyl methacrylate) (mPEG-*b*-P(APNBMA)<sub>n</sub>) diblock copolymer consists of a non-fouling poly(ethylene glycol) (PEG) block and a biocompatible cationic polymer block. The cationic charges provide efficient electrostatic binding to encapsulate siRNA. Polyplexes self-assemble in aqueous solution due to electrostatic interactions. Within the cationic polymer block, a photo-cleavable *o*-nitrobenzyl group is incorporated. Upon ultraviolet (UV) irradiation the *o*-nitrobenzyl group cleaves to form a negatively charged carboxylate ion.<sup>15</sup> The cleavage breaks apart the polyplex structure when and where photo-stimulus is applied, leading to spatiotemporal control over siRNA release. Previous results show that the photo-responsive polyplexes do not disassemble without UV light, demonstrating complete spatiotemporal control over siRNA delivery.<sup>17</sup> Additionally, the photo-responsive polyplex enables delivery of precise doses of siRNA due to tight packing with the cationic charges on the polymer and sufficient release upon charge reversal. The photo-responsive polyplex system simultaneously and independently controls siRNA encapsulation and release. Figure 1-1 shows the mPEG-*b*-P(APNBMA)<sub>n</sub> as well as the self-assembly of the polyplexes.

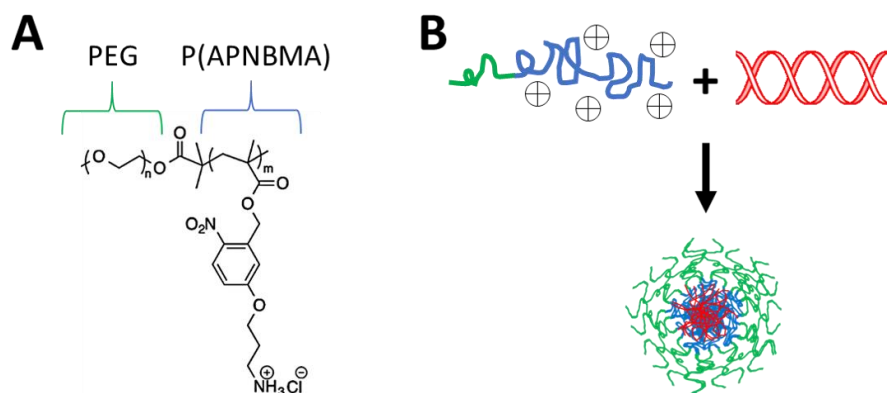


Figure 1-1. Photo-responsive polyplexes. A) Diblock copolymer mPEG-*b*-P(APNBMA)<sub>n</sub> structure. B) Photo-responsive polyplex assembly.

## 1.5 Thesis summary

The work herein uses the photo-responsive polyplex system developed by the Epps and Sullivan groups to explore efficient and controlled methods of siRNA delivery by pursuing three specific research aims:

- 1) Optimize polyplex formulations by mixing two polymers of different lengths rather than synthesizing a library of polymers
- 2) Incorporate kinetic modeling to optimize siRNA dose schedule and improve research process efficiency
- 3) Deliver multiple siRNAs in a single polyplex by developing layered polymer nanocarriers

The materials and methods used in this research are outlined in Chapter 2. Advances made towards Research Aim 1 and Aim 2 are discussed in Chapter 3. Therein, the process of mixing short ( $n = 7.9$ ) and long ( $n = 23.6$ ) strands of mPEG-*b*-P(APNBMA)<sub>n</sub>, polyplex composition is optimized for maximal gene silencing upon a single dose of siRNA. Additionally, simple kinetic modeling is incorporated to

develop a dosing schedule for siRNA.<sup>18</sup> Chapter 4 discusses approaches towards Research Aim 3. A method for formulating photo-responsive layered nanocarriers is demonstrated, and suggestions for future directions of the layered nanocarrier project are suggested. The work herein makes several advances towards improved siRNA delivery efficiency with photo-responsive polyplex systems.

## Chapter 2

### MATERIALS AND METHODS

#### 2.1 Materials

The mPEG-*b*-P(APNBMA)<sub>n</sub> ( $M_n = 7,900 \text{ g mol}^{-1}$ ,  $n = 7.9$ ;  $M_n = 13,100 \text{ g mol}^{-1}$ ,  $n = 23.6$ ) polymers were synthesized *via* atom-transfer radical polymerization as described in previous work.<sup>15</sup> All siRNA molecules were purchased from GE Healthcare Dharmacon, Inc. (Chicago, IL). ON-TARGETplus non-targeting siRNAs and anti-GAPDH siRNAs were used as received. Custom-made siRNA (both Dy547- and Dy647-labeled) targeting GAPDH were designed and altered terminally with 5'-P and a fluorophore (sense: 5' Dy547/Dy647-GUGUGAACACGAGAAAUAUU 3'; antisense: 5' 5'-P-UAUUUCUCGUGGUUCACACUU 3'). Dulbecco's modification of Eagle's medium (DMEM) and PBS (150 mM NaCl) were obtained from Corning Life Sciences – Mediatech Inc. (Manassas, VA). Opti-MEM® media, SuperSignal™ West Dura Chemiluminescent Substrate and TRIzol® Reagent were purchased from Thermo Fisher Scientific (Waltham, MA). Bovine serum albumin (BSA) and a bicinchoninic acid (BCA) protein assay kit were purchased from Pierce (Rockford, IL). The anti-GAPDH and secondary HRP antibodies were purchased from AbCam (Cambridge, MA). The anti-actin antibody was purchased from Santa Cruz Biotechnology (Dallas, TX). Primers were obtained from Eurofins MWG Operon (Huntsville, AL) with the following sequences: GAPDH forward 5' CGGGTTCCTATAAATACGGACTGC 3'; GAPDH reverse 5'

CCCAATACGGCCAAATCCGT 3';  $\beta$ -actin forward 5' CTGTCGAGTCGCGTCCA 3';  $\beta$ -actin reverse 5' TCATCCATGGCGAACTGGTG 3'. The iTaq<sup>TM</sup> Universal SYBR<sup>®</sup> Green One-Step Kit and optical flat 8-cap strips were purchased from Bio-Rad (Hercules, CA). All other reagents were obtained from Thermo Fisher Scientific (Waltham, MA).

## 2.2 Methods

### 2.2.1 Single-layer polyplex nanocarrier formulation

Polyplexes were formulated *via* self-assembly method by using solution mixing followed by gentle vortexing. Solutions of siRNA were prepared at 32  $\mu\text{g mL}^{-1}$  in 20 nM 4-(2-hydroxyethyl)piperazine-1-ethanesulfonic acid (HEPES) buffer at pH 6.0. Polymer solutions were prepared in HEPES buffer by adding appropriate amounts of mPEG-*b*-P(APNBMA)<sub>7.9</sub> and mPEG-*b*-P(APNBMA)<sub>23.6</sub> to vary the molar charge compositions of each polymer as desired. The polymer solutions were added to equal volumes of siRNA solutions to achieve the desired total N/P ratios (N: amine groups on polymers, P: phosphate groups on siRNA). The polymer solution was slowly added while gently vortexing over a period of 10 s. Polyplexes were incubated for 30 min at room temperature in a dark environment before performing additional experiments.

### **2.2.2 Multi-layer polyplex nanocarrier formulation**

Methods for developing layered polyplex nanocarriers for delivering multiple siRNAs is discussed in detail in Chapter 4.

### **2.2.3 Ethidium bromide gel electrophoresis**

Polyplexes were formulated as described and subjected to gel electrophoresis. Gels were prepared with 2 wt.% agarose and stained with  $0.5 \mu\text{g mL}^{-1}$  ethidium bromide. To analyze polyplexes,  $12.5 \mu\text{L}$  of polyplex solution was added to  $2.5 \mu\text{L}$  of gel loading solution (3:7 (v/v) glycerol/water) before being added to the wells. Gels were run at 100 V for 30 min and imaged using a Bio-Rad Gel Doc XR (Hercules, CA). ImageJ software was used to quantify the amounts of free siRNA by analyzing the intensities of the fluorescent siRNA bands in the gel.

### **2.2.4 Photo-responsive siRNA release**

Polyplexes were incubated in sodium dodecyl sulfate (SDS) solutions at an S/P ratio of 2.5 (S: sulfate groups on SDS, P: phosphate groups on siRNA) at room temperature in a dark environment for 30 min. Then,  $62.5 \mu\text{L}$  of polyplex solution was sealed between two glass slides and enclosed by a rubber barrier on each side. The polyplex solutions were subjected to irradiation with 365 nm light at  $200 \text{ W/m}^2$  for varying amounts of time (0-40 min). A sample of  $12.5 \mu\text{L}$  of polyplex solution was collected from the glass slides at each desired time point. The amount of released siRNA was quantified *via* the gel electrophoresis techniques described previously.

## **2.2.5 Polyplex size determination**

### **2.2.5.1 Fluorescence correlation microscopy (FCS)**

Average polyplex diameters were determined initially *via* fluorescence correlation spectroscopy (FCS) analysis. Polyplexes were formulated with Dy547-labeled siRNA and placed on cover slips, which were subsequently attached to a glass microscope slide by SecureSeals from Life Technologies (Grand Island, NY). FCS measurements were performed on an LSM 780 confocal microscope (Carl Zeiss, Oberkochen, Germany) using a 488 nm laser and a 40x (numerical aperture [NA] = 1.2) water immersion apochromat objective. Thirty measurements, each lasting 8 s, were taken for each sample. Data analysis was performed with ZEN 2010 software (Carl Zeiss). The structural and measurement parameters were determined using a solution of AlexaFluor555 dye with an assumed diffusion coefficient of  $340 \mu\text{m}^2 \text{s}^{-1}$ . Chad Greco performed these experiments.

### **2.2.5.2 Dynamic light scattering (DLS)**

Dynamic light scattering (DLS) was used to confirm the size of the polyplexes determined *via* FCS. Additionally, all size measurements for the layered polyplex nanocarriers were determined by DLS. Polyplex solutions were diluted in HEPES to a total volume of 400  $\mu\text{L}$  in glass test tubes and capped with Parafilm to keep out dust and other contaminants. Measurements were taken for 1 min for each sample of polyplexes.

### **2.2.6 Determining charge with zeta potential**

Polyplex solutions were prepared as described and diluted with HEPES buffer to a volume of 1 mL. The solutions were then transferred to a cuvette and analyzed using a ZetaPALS zeta potential analyzer from Brookhaven Instruments (Brookhaven, CT). The samples were measured at 25 °C, and the Smoluchowski model was used to analyze the data. Reported values were computed as the average of three independent experiments comprising 10 measurements each.

### **2.2.7 Cell culture and transfection**

NIH/3T3 cells were purchased from the American Type Culture Collection (ATCC, Manassas, VA). The cells were cultured in DMEM supplemented with 10 vol% fetal bovine serum and 1 vol% penicillin-streptomycin. The cells were maintained at 37 °C in a humidified environment with 5 vol% CO<sub>2</sub>. For transfections, cells were plated in 6 well plates at a density of 100,000 cells per well. The cells could adhere and recover for 24 h. In preparation for transfection, DMEM was removed, PBS was added in a wash step, and Opti-MEM® reduced serum media was added. Polyplex solutions at an N:P ratio of 4 were added to a final siRNA concentration of 20 nM, and the cells were incubated for 3 h. Following transfection, all cells were washed with PBS and incubated in fully supplemented media for 30 min. For samples undergoing UV light treatment, the media was removed and replaced with Opti-MEM® without phenol red. The cells were subsequently irradiated with 365 nm

light at an intensity of 200 W/m<sup>2</sup> for 10 min while on a 37 °C hot plate. Cells were then incubated in fully supplemented DMEM for the remainder of the culture duration.

### **2.2.8 Cellular uptake**

Cells were seeded in 12-well plates at a density of 40,000 cells per well and could adhere and recover for 24 h. Polyplex solutions were formed with Dy647-labeled siRNA, which were then delivered to cells following the previously described transfection protocol. After the 3 h transfection, cells were washed with PBS solution and prepared for flow cytometry analysis following standard trypsin-based protocols. The cells were resuspended in PBS solution and filtered in a 35 µm nylon mesh filter to remove aggregates in solution. The cells were stored on ice until further analysis. An Accuri C6 instrument (BD Biosciences, San Jose, CA) was used to collect flow cytometry measurements. The analysis was conducted about 4.5 h post transfection, and at least 10,000 live cells were analyzed per sample. FlowJo software was used to analyze the data and quantify the mean fluorescence intensity per cell.

### **2.2.9 Gene silencing analysis**

Western blot analyses were used to measure GAPDH protein silencing. In the single dose experiments, cells were transfected as described. Then, 48 h after the start of transfection, protein was extracted from the cells by adding a lysis solution composed of 0.5 vol% Triton X-100, 0.5% sodium deoxycholate, 150 mM NaCl, 5 mM Tris-HCl (pH 7.4), 5 mM EDTA, and 1x Halt Protease and Phosphatase Inhibitor

cocktail. For the repeated dosing experiments, a second transfection of polyplexes occurred 28 h after the first transfection process. Protein was extracted with cell lysis solution 75 h after the start of the first transfection. The total protein concentration of each sample was measured using the BSA Protein Assay Kit. The protein solutions were then subject to 4% - 20% sodium dodecyl sulfate polyacrylamide gel electrophoresis (SDS-PAGE) for 35 min at 150 V. The separated proteins were then transferred onto a poly(vinylidene fluoride) membrane at 18 V for 75 min. The membrane was subsequently blocked in 5 vol % BSA in Tris-HCl-buffered saline (50 mM Tris-HCl, pH 7.4, 150 mM NaCl) containing 0.1 vol % Tween 20 (TBST) at room temperature for 1 h. The membrane was incubated overnight with anti-GAPDH rabbit monoclonal IgG primary antibody in TBST at 4 °C. The next day, the membrane was incubated with a solution of secondary goat anti-rabbit polyclonal IgG antibody conjugated to horseradish peroxidase (HRP) for 1 h. The SuperSignal™ West Dura Chemiluminescent Substrate was used to image the GAPDH bands, which were then quantified using ImageJ software. The membrane was stripped for 15 min with Restore™ PLUS Western Blot stripping buffer and blocked in BSA solution for 1 h. The membrane was incubated with anti-actin rabbit monoclonal IgG primary antibody overnight. The following day, the same secondary antibody and imaging techniques were used to measure the actin bands. ImageJ was used to analyze the intensity of the protein bands on the image.

### **2.2.10 mRNA silencing**

GAPDH mRNA knockdown was measured using qPCR. Single and double transfections were carried out as described previously and RNA was isolated by TRIzol® Reagent according to the manufacturer's protocols 48 h and 75 h post-transfection, respectively. The iTaq™ Universal SYBR® Green One-Step Kit and the specific GAPDH and  $\beta$ -actin primers were used to prepare samples in triplicate as described in the manufacturer's protocols. The cDNA synthesis and qPCR steps were conducted on a Bio-Rad CFX96™ using the following conditions: 10 min at 50 °C; 1 min at 95 °C; 40 cycles of 10 s at 95 °C and 30 s at 60 °C, and finally a 65 °C to 95 °C ramp at 0.5 °C increment steps every 5 s. The  $\Delta\Delta$ CT method was used for fold change analysis,<sup>48</sup> and all test sample data were normalized to untreated cell data. The mRNA knockdown studies were conducted by Chad Greco.

### **2.2.11 Kinetic modeling**

A simple kinetic model was used to simulate the dynamic silencing response and relative cellular concentrations of siRNA, mRNA, and protein. A system of ordinary differential equations was used to model the changes in concentrations of each of the three biomolecules. Rate constants were computed based on the component half-lives reported in literature<sup>19,20</sup> and fit to ensure mRNA and protein steady-state values were reached in the absence of siRNA. The set of equations was solved using differential equation solver ode45 in MATLAB. Relative concentrations

of mRNA and protein were normalized to 100 as original values, and siRNA release was modeled as 100 relative units after application of UV light.

## Chapter 3

### COMBINING MIXED POLYMER NANOCARRIERS WITH SIMPLE KINETIC MODELING TO TUNE siRNA DOSE RESPONSE

The content in Chapter 3 is modified from Greco and Muir et. al.<sup>18</sup>

#### 3.1 Background and motivation

##### 3.1.1 Mixed polyplexes

Synthesizing a library of polymers is the most common approach in optimizing polyplex delivery systems.<sup>11,21</sup> However, taking the time and resources to synthesize multiple polymers and analyze each one for siRNA delivery efficiency can be a time-consuming and costly process. A more efficient approach is to optimize polyplex formulations by creating mixed polyplexes, which contain as little as two different polymer components. The ratio of polymer components within a single polyplex is optimized rather than synthesizing multiple materials for analysis. Parameters like size and charge of the polyplexes can be tuned by altering ratios of as little as two different polymers.<sup>22</sup> For example, Duvall et. al. demonstrated an approach to tuning siRNA delivery by creating mixed micelles and altering the ratios of two diblock copolymers with different amounts of PEG.<sup>23</sup> They found that while increasing PEG content decreased cellular internalization due to decreased cationic charge density, it also increased the amount of intracellular unpackaging of siRNA, thus delivering more siRNA per internalized polyplex.

##### 3.1.2 Kinetic modeling and dosing schedule

Biomedical research is often approached with a “trial and error” method in terms of selecting time intervals for sampling and developing dosing schedules. The

field of pharmacokinetic modeling is developing with the advancements in physiologically-based pharmacokinetic (PBPK) techniques to incorporate simple kinetic models for biomolecule distribution at the organ system, tissue, and cellular level.<sup>24</sup> Bringing computational modeling into the research process reduces time and material resources, and it also has potentials to reduce the number of animals required for research experiments.

Kinetic modeling in siRNA dosing requires knowledge of many parameters, including siRNA, mRNA, and protein half-lives, as well as specific kinetics of the release mechanism of the delivery system. Many systems rely on commercial siRNA delivery agents like Oligofectamine® and Lipofectamine®, which do not have a controlled on/off mechanism for siRNA release and complicate kinetic modeling.<sup>20,25</sup> Coupling kinetic modeling with an externally controlled siRNA delivery vehicle will simplify kinetic modeling efforts and lead to more accurate predictive siRNA dose response. Photo-responsive siRNA delivery provides excellent on/off control of siRNA release, which simplifies the kinetic modeling process and enables more accurate predictions of siRNA dosing.

### **3.2 Research Aims 1 and 2 – Mixed polyplexes combined with kinetic modeling**

This chapter discusses efforts to combine the mixed polyplex approach with simple kinetic modeling to optimize siRNA delivery efficiency in the photo-responsive polyplex system.<sup>18</sup> Two mPEG-*b*-P(APNBMA)<sub>n</sub> polymers were synthesized – a short polymer, with  $n = 7.9$ , and a long polymer, with  $n = 23.6$ . Figure 3-1 depicts a schematic representation of the mixed polyplex system. Polyplexes were named as a molar ratio of the short/long polymer. For example, a 25/75 polyplex has a 0.25 molar fraction of short polymer and a 0.75 molar fraction of longer polymer. It

was found that the longer polymer demonstrated stronger siRNA binding, yet the shorter polymer demonstrated enhanced siRNA release. Polyplexes with a 50/50 ratio were shown to have the highest cellular uptake and maximum gene silencing abilities. Furthermore, simple kinetic modeling was incorporated to predict a dosing schedule for a single and double dose of photo-responsive siRNA polyplexes. The work in this chapter demonstrates promising efforts towards Research Aims 1 and 2 for the project.

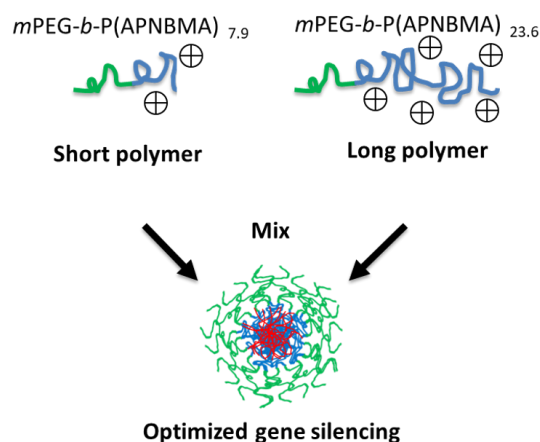


Figure 3-1. Mixed polyplex structure.

### 3.3 Results and discussion

#### 3.3.1 Mixed polyplex siRNA encapsulation

Efficient binding and encapsulation of siRNA is required for a polymer delivery vehicle to protect siRNA from being damaged or degraded before cellular uptake.<sup>11</sup> To analyze the encapsulation abilities of the mixed polyplexes, ethidium

bromide gel electrophoresis assays were conducted. As shown in Figure 3-2, all polyplexes fully encapsulated siRNA at a total N:P  $\geq 1.5$ . At total N:P ratios of 0 to 1, there was a clear increase in the percent of free siRNA as more mPEG-*b*-P(APNBMA)<sub>7.9</sub> was added to the polymer mixture. This aligns with the previously demonstrated trend of slightly enhanced encapsulation abilities of the mPEG-*b*-P(APNBMA)<sub>23.6</sub> polymer.<sup>17</sup> Moving forward, all polyplexes were made at a total N:P of 4 to ensure complete encapsulation of siRNA.

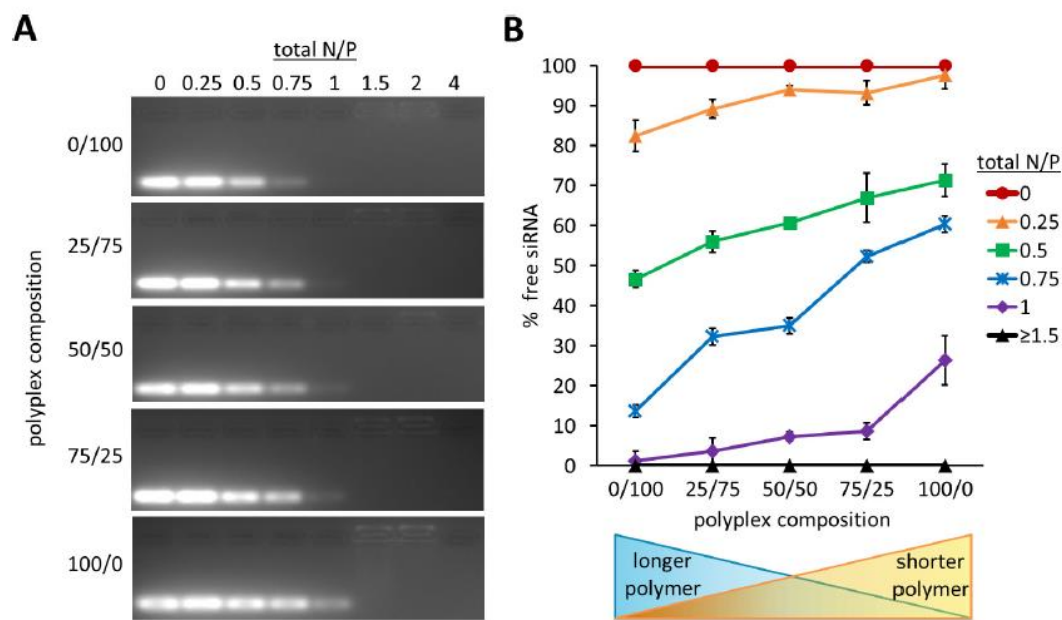


Figure 3-2. Gel electrophoresis assay of mPEG-*b*-P(APNBMA)<sub>n</sub>/siRNA polyplexes. A) Gel electrophoresis of polyplexes formed at varying total N:P ratios. B) Quantification of gel electrophoresis images based on ImageJ analysis of siRNA bands. Figure is reprinted from Greco and Muir et. al. with permissions from Elsevier.<sup>18</sup>

### 3.3.2 Gene silencing

Because the cationic charge density and length of a polymer has been shown to significantly affect gene silencing efficiencies,<sup>26</sup> we hypothesized that mixtures of the two polymers would possess different abilities to mediate RNAi. Furthermore, mixing two polymers to optimize siRNA release is a more efficient process than synthesizing a large polymer library and experimenting with each polymer. Thus, mixed polyplexes containing siRNA targeting glyceraldehyde 3-phosphate dehydrogenase (GAPDH) were delivered to mouse embryonic fibroblast (NIH/3T3) cells. The cells were treated with 365 nm light for 10 min, and changes in GAPDH protein expression levels were measured 48 h post-transfection. As shown in Figure 3-3, the 0/100 polyplexes exhibited ~40% knockdown, which was consistent with previous work.<sup>17</sup> Furthermore, all mixed polyplex systems showed an increased ability to mediate gene knockdown. Polyplexes containing an equimolar charge ratio of the two polymers demonstrated the highest gene silencing capabilities with ~70% knockdown achieved. This level of silencing has been shown to be approximately the highest degree of knockdown achievable with a single dose of siRNA due to the relatively long half-life of the GAPDH protein.<sup>19</sup> However, the level of silencing decreased as even more mPEG-*b*-P(APNBMA)<sub>7.9</sub> chains were incorporated. Additionally, cells transfected with any of the polyplex formulations, but not treated with UV light, exhibited no silencing, which demonstrates that all the polyplex systems remained dormant in the cell without treatment of the photo-stimulus, providing on/off control of siRNA activity. The complete dormancy of the polyplexes without UV stimulus was

surprising, given that many other siRNA delivery systems will rapidly degrade in the extracellular environment and exhibit un-controlled release of siRNA.<sup>27</sup> The result demonstrates the enhanced stability of the photo-responsive polyplexes in intracellular environments, likely due to cooperative electrostatic and hydrophobic interactions.<sup>16</sup> Stability is required to eliminate off-target effects and unwanted immune responses,<sup>28</sup> which demonstrates the viability of our polyplex system.

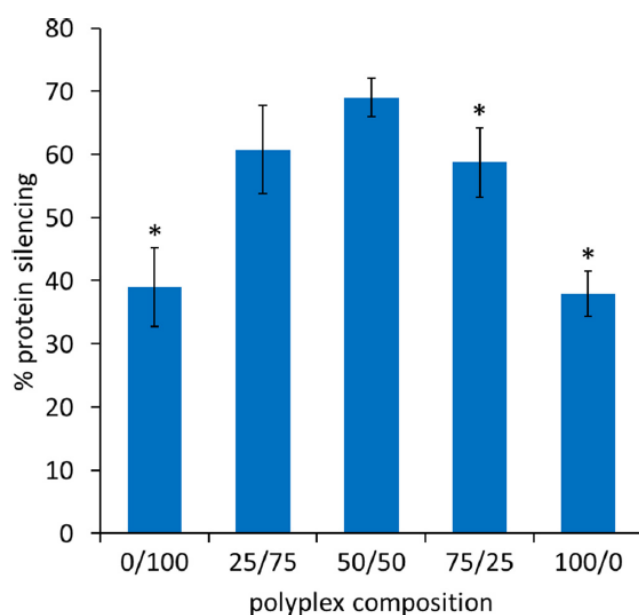


Figure 3-3. GAPDH protein expression levels as a function of molar composition of  $m\text{PEG-}b\text{-P}(\text{APNBMA})_{7.9} / m\text{PEG-}b\text{-P}(\text{APNBMA})_{23.6}$ .<sup>18</sup> Cells were treated with siRNA polyplexes and subsequently exposed to UV light for 10 min and lysed for western blot analysis 48 h post-transfection. Data represent the GAPDH protein expression levels relative to the levels of the loading control  $\beta$ -actin, normalized to the native protein levels in controls with no siRNA treatment. Results are shown as the mean  $\pm$  standard deviation of data obtained from three independent experiments. Statistical significance compared to the 50/50 formulation is marked with an “\*”. Figure is reprinted from Greco and Muir et. al. with permissions from Elsevier.<sup>18</sup>

### 3.3.3 Light-induced siRNA release

Polymer delivery vehicles for siRNA must meet contradictory demands for efficient siRNA binding and siRNA release. To assess the degree of siRNA released, polyplexes were formulated and then incubated in a solution of sodium dodecyl sulfate (SDS) to simulate intracellular environments containing lipids. The samples were irradiated with light for varying lengths of time, and the percentage of free siRNA was visualized using gel electrophoresis and quantified with ImageJ analysis. As shown in Figure 3-4, as the amount of mPEG-*b*-P(APNBMA)<sub>7.9</sub> in the polyplexes increased, the amount of siRNA released from UV exposure slightly increased. This trend is consistent with the encapsulation study and indicated that mPEG-*b*-P(APNBMA)<sub>23.6</sub> has a higher binding affinity for siRNA. However, the increase in the percentage of siRNA released is contradictory to the decrease in gene silencing measured for the 75/25 and 100/0 polyplexes. Therefore, we hypothesized that the total amount of siRNA being internalized into the cells must be different to explain the trends in gene silencing.

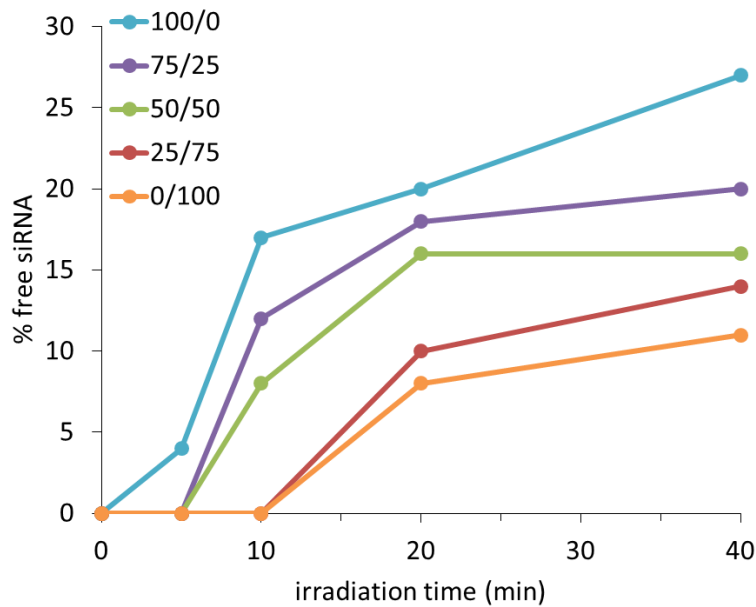


Figure 3-4. Light-mediated release of siRNA from mPEG-*b*-P(APNBMA)<sub>n</sub>/siRNA polyplexes.<sup>18</sup> Polyplexes were formed at an N:P of 4 and exposed to SDS solutions at an S:P of 2.5 before being irradiated with UV light for 10 min. The amount of free siRNA was quantified *via* ImageJ analysis of gel electrophoresis experiments. Figure is reprinted from Greco and Muir et. al. with permissions from Elsevier.<sup>18</sup>

### 3.3.4 Cellular uptake

To investigate if the level of cellular uptake was playing a role in determining the gene silencing trends, NIH/3T3 cells were transfected with mixed polyplexes containing fluorescently labeled siRNA. Flow cytometry was used to analyze the relative fluorescence intensities of transfected cells, which provided information about the relative uptake of each mixed polyplex system. As shown in Figure 3-5, polyplexes made from a mixture of the two polymers showed enhanced cellular uptake. Specifically, the 50/50 polyplexes showed the highest level of cellular uptake with a normalized mean fluorescence intensity (MFI) of ~160%; i.e. 60% more 50/50

polyplexes were taken up relative to 0/100 polyplexes. As is apparent visually, the trend in MFI closely matched the trend of gene silencing. Therefore, the effect of mixed polyplexes on cellular uptake is the dominant reason for enhanced gene silencing of mixed polyplexes, though the amount of light-induced siRNA release likely also contributes to a lesser degree. A greater number of siRNAs pass through the cellular membrane, and thus more siRNA is available to cleave mRNAs upon escape into the cytoplasm.

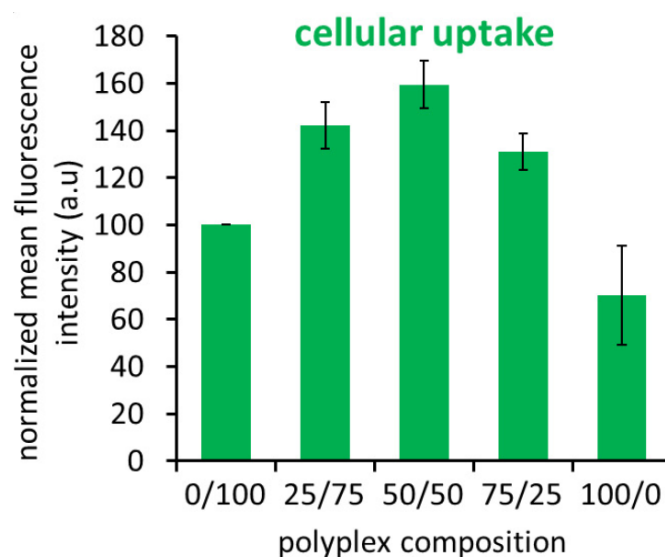


Figure 3-5. Cellular uptake of mPEG-*b*-P(APNBMA)<sub>n</sub>/siRNA polyplexes.<sup>18</sup> Fluorescently tagged siRNA was incorporated into polyplexes and delivered to cells for flow cytometry analysis. The mean fluorescence intensity per cell was normalized to the 0/100 polyplexes. Results are shown as the mean  $\pm$  standard deviation of data obtained from three independent samples. Figure is reprinted from Greco and Muir et. al. with permissions from Elsevier.<sup>18</sup>

### 3.3.5 Polyplex size and charge

The extent of cellular uptake has been reported to be dependent on the size and zeta potential of the nanocarrier.<sup>26</sup> Thus, we hypothesized that the combination of these properties was determining the ability of polyplexes to be internalized into cells. Most delivery systems have aimed for attaining smaller sizes, which are thought to be beneficial for more rapid uptake. Using fluorescence correlation spectroscopy (FCS), the average diameter of each mixed polyplex was measured. As shown in Figure 3-6, the 0/100 polyplexes had a diameter of ~120 nm, which was consistent with DLS measurements reported previously.<sup>16</sup> Adding more mPEG-*b*-P(APNBMA)<sub>7.9</sub> to the polyplex system decreased the diameter, and the 100/0 polyplexes had a diameter of only ~25 nm. Therefore, polyplexes with greater amounts of mPEG-*b*-P(APNBMA)<sub>7.9</sub> would be expected to be internalized more efficiently.

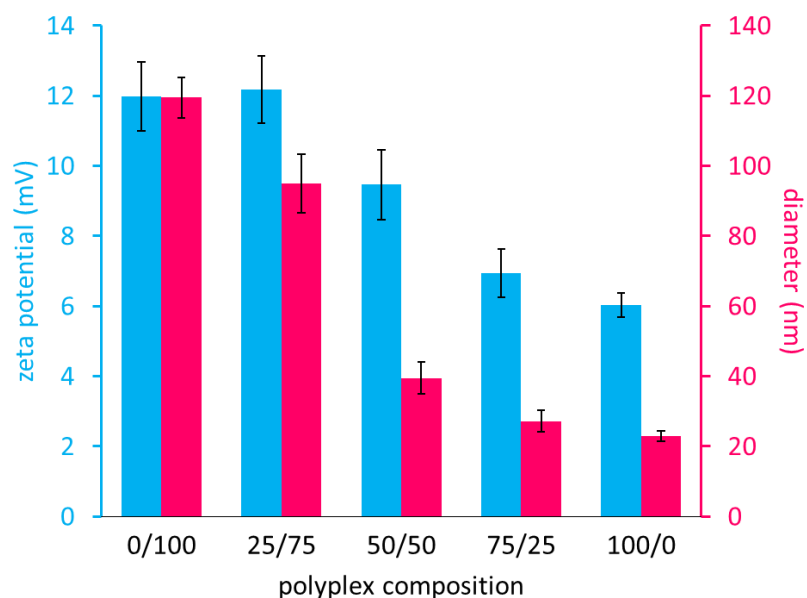


Figure 3-6. Average zeta potentials (light blue, associated with primary y-axis) and diameters (pink, associated with secondary y-axis) of polyplexes with varying compositions.<sup>18</sup> Polyplexes were formed at a total N:P of 4, with different polymer compositions of mPEG-*b*-P(APNBMA)<sub>7,9</sub>/mPEG-*b*-P(APNBMA)<sub>23,6</sub>, on a molar basis of cationic amine groups. Results are shown as the mean  $\pm$  standard deviation of data obtained from three independent measurements. Figure is reprinted from Greco and Muir et. al. with permissions from Elsevier.<sup>18</sup>

The zeta potential was measured for each formulation and is plotted in Figure 3-6. The positive zeta potential values indicate that all the polyplexes had an overall moderately positive net charge, which was expected based on the excess polymers used in the formulation (total N:P of 4) and the presence of a PEG shielding layer. However, as the percentage of mPEG-*b*-P(APNBMA)<sub>7,9</sub> increased, the zeta potential decreased. The zeta potential decrease is most likely the result of increased shielding of the positive polyplex core due to the inclusion of polymers with higher mass

fractions of PEG. Higher zeta potentials are preferred for transportation across the anionic cellular membrane due to attractive electrostatic forces.<sup>26</sup> The low zeta potential (~2 mV) of the 100/0 polyplexes explains their lower cellular uptake despite their small size. The 50/50 polyplexes fall in the middle with a relatively high zeta potential of ~10 mV and a small diameter of ~40 nm. It also is important to note that a single population of polyplexes was detected for each formulation, suggesting that each polyplex was comprised of proportional amounts of each polymer. Mixed polyplexes balance the need for high zeta potential and small diameter. The optimization of these two properties explains the greatly enhanced cellular uptake of mixed polyplex systems.

### **3.3.6 Kinetic modeling**

#### **3.3.6.1 Single polyplex dose**

Advances in biomaterial design can be paired with developments in kinetic modeling to gain a better understanding of the dynamic silencing response to achieve optimal gene knockdowns and guide dosing regimens. Previously, we reported that 0/100 polyplexes required 20 min of irradiation to achieve 70% knockdown (to reduce GAPDH protein levels to ~30%).<sup>16</sup> Furthermore, this degree of silencing was shown to be the maximum achievable level with a single transfection due to the relatively long GAPDH protein half-life, as supported through experimental evidence and mass action kinetic modeling. In this work, we determined that the 50/50 polyplexes

mediated the same level of maximum knockdown efficiency following only 10 min of light treatment; thus, we chose to use the 50/50 formulation moving forward.

We sought to demonstrate with kinetic modeling that the 50/50 polyplex system was achieving the maximum level of GAPDH silencing possible upon a single dose of siRNA. The dynamic silencing process is governed by fundamental biological rates, such as cell doubling time and protein and mRNA half-lives. Therefore, these parameters directly affect the maximum gene silencing efficiencies for each system with a single dose of siRNA. To demonstrate the dynamic silencing process, a simple system of ordinary differential equations was solved using rate constants determined through literature values of protein half-lives and cell doubling times.<sup>19,20</sup> The simple model is advantageous in because the model enables easy implementation compared to other relatively complicated models in the literature,<sup>29</sup> which makes the model more likely to be adopted on a large scale. Additionally, the model was able to be streamlined only because our polyplexes exhibited precise control over the timing of siRNA release.

As shown in Figure 3-7A, the mRNA and protein levels maintained their steady-state values before the introduction of siRNA, which was controllably released following light exposure at 3.5 h post-transfection. A rapid decrease in the mRNA levels was apparent immediately, followed by the slower decrease of the protein levels. The amount of siRNA decreased with time, primarily due to dilution through cell division. Consequently, the mRNA levels reached a minimum level of <10% and

started to recover, which caused the protein levels to plateau at ~36% before they started to increase after 48 h post-transfection.

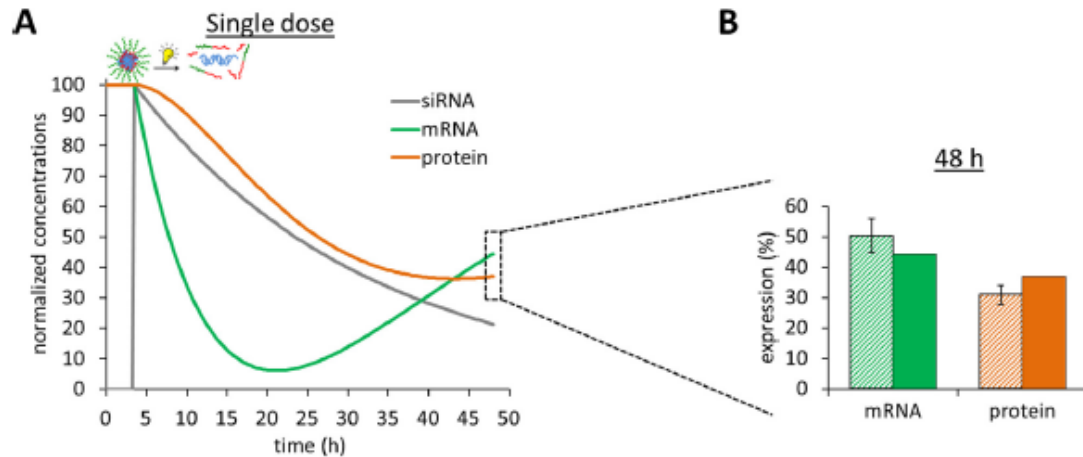


Figure 3-7. Mass action kinetic models predict the dynamic nature of the GAPDH silencing process with a single dose (A) of siRNA.<sup>18</sup> Initial protein and mRNA concentrations were normalized to 100 to simulate steady-state conditions. After application of UV light, 100 normalized units of siRNA were introduced. The UV light was applied 3.5 h after each transfection. B) Cells were lysed at 48 h following either a single dose of siRNA. GAPDH mRNA and protein expression levels were determined through qPCR and western blot experiments, respectively. Model predictions of mRNA (green) and protein (orange) expression levels at the end points of 48 h are presented as solid bars; experimental values are presented as diagonal striped bars. Experimental values are shown as the mean  $\pm$  standard deviation of data obtained from three independent samples. Figure is reprinted from Greco and Muir et. al. with permissions from Elsevier.<sup>18</sup>

As depicted in Figure 3-7B, the kinetic model accurately captured the determined experimentally protein expression levels of the dynamic silencing response of the 50/50 polyplexes from Figure 3-3. Additionally, the model predicted mRNA

levels to be ~45%. To further validate the model, qPCR measurements were taken and found to agree with the model prediction. Notably, the results demonstrate the ability to achieve a level of silencing of ~70% knockdown of GAPDH with a single dose of siRNA, which was previously shown to correspond to RISC saturation.<sup>17</sup> Additionally, we used an siRNA concentration of 20 nM, which is significantly lower than concentrations used by many similar polyplex systems in literature (typically 100 nM).<sup>27</sup> The enhanced efficiency of the 50/50 polyplexes, combined with the ability to control the timing of siRNA release precisely, allowed for the development of a predictable and effective siRNA dosing schedule to silence an endogenous protein with a relatively long half-life.

### **3.3.6.2 Repeated polyplex dose and predictive dosing schedule**

Though the siRNA-mediated silencing process is dynamic in nature, most literature reports fail to consider crucial kinetic factors governing the silencing response such as mRNA and protein half-lives. Oftentimes, incomplete knockdown is attributed to limitations of the delivery vehicle and further dosing is not pursued due to concerns with cytotoxicity. As we reported previously, cells treated with polyplex solutions and 20 min of irradiation maintained excellent viability. Given that the 50/50 polyplexes required only half of the irradiation time to maximize silencing, we hypothesized that applying a second dose of siRNA would enable further knockdown of protein without compromising cell viability. Numerous dosing schedules were generated by the model to determine the optimal time to deliver the second dose of

siRNA. The model predicted that polyplexes delivered at 28 h post-transfection followed by UV light irradiation 3.5 h later would result in significantly enhanced protein knockdown before levels started to recover ~75 h post-transfection (Figure 3-8A). To test the validity of the kinetic model, mRNA and protein expression levels were measured at 75 h post-transfection and are shown in Figure 3-8B. These determined experimentally values were in excellent agreement with the model predictions. The protein expression was ~15%, which is half of the level achievable by a single dose (~30%), which demonstrated that multiple dosing was a successful method for further silencing GAPDH beyond the maximum achievable levels of a traditional single dose. Additionally, it is important to note that these predictions were made possible only because our nucleic acid delivery system is capable of precise and timely control over siRNA release.

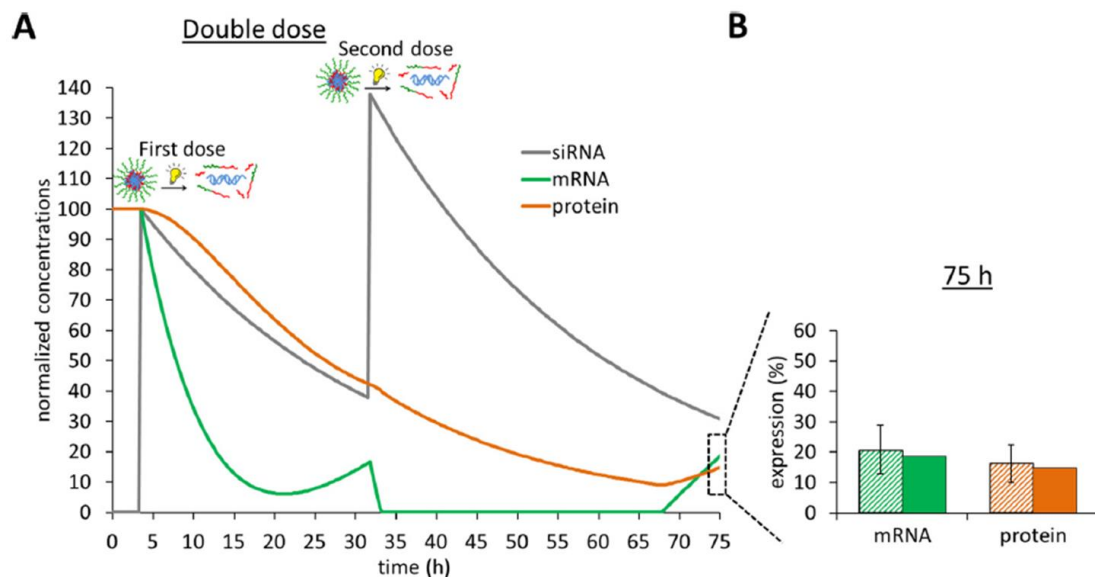


Figure 3-8. Mass action kinetic models predict the dynamic nature of the GAPDH silencing process with a double dose of siRNA.<sup>18</sup> Initial protein and mRNA concentrations were normalized to 100 to simulate state-state conditions. After application of UV light, 100 normalized units of siRNA were introduced. The UV light was applied 3.5 h after each transfection. B) Cells were lysed at 75 h following either a double dose of siRNA. GAPDH mRNA and protein expression levels were determined through qPCR and western blot experiments, respectively. Model predictions of mRNA (green) and protein (orange) expression levels at the end points of 75 h are presented as solid bars; experimental values are presented as diagonal striped bars. Experimental values are shown as the mean  $\pm$  standard deviation of data obtained from three independent samples. Figure is reprinted from Greco and Muir et. al. with permissions from Elsevier.<sup>18</sup>

### 3.4 Conclusions

We have demonstrated that the simple mixing of two photo-responsive polymers with different cationic block lengths resulted in dramatic changes in siRNA delivery efficiencies. Mixtures of mPEG-*b*-P(APNBMA)<sub>n</sub> polymers containing the same hydrophilic block, but different lengths of the cationic block, self-assembled with

siRNA to form stable nanocarriers. All these polyplexes maintained dormancy without application of light. However, upon exposure to the photo-stimulus, the 50/50 polyplex formulations were shown to knockdown GAPDH protein most effectively and achieve a maximum gene silencing efficiency of 70%. Though nanocarriers with increasing amounts of the shorter cationic block released greater amounts of siRNA after irradiation with light, the level of cellular uptake was shown to be the dominant characteristic determining the extent of gene silencing. Polyplexes composed of equimolar charge ratios of each polymer provided the best uptake by balancing size and surface charge effects. Additionally, the most efficient carriers capable of precisely controlled siRNA release were used to test a mass action kinetic model. The model accurately predicted mRNA and protein expression levels following a single dose of siRNA. Furthermore, a dosing regimen was developed to maximize silencing of a relatively stable protein, GAPDH. The optimized mixed polyplex system shows complete encapsulation siRNA and efficient release of siRNA which makes development of a kinetic model possible and accurate. The predicted levels of silencing were confirmed through experimental data and double dosing of siRNA knocked down protein expression to half of the maximum level achievable with a single dose. Additionally, our groups have demonstrated that the simple kinetic model can be extended to predict silencing of multiple proteins in different cell lines, demonstrating the versatility and high-impact of the simple model.<sup>17,30</sup> Thus, the development of the mixed polyplex system combined with simple kinetic modeling

approaches demonstrates significant progress towards Research Aims 1 and 2 in the work herein.

## Chapter 4

### LAYERED NANOCARRIERS FOR SEQUENTIAL RELEASE OF MULTIPLE siRNAs

#### 4.1 Background and motivation

##### 4.1.1 Controlled delivery of multiple doses of siRNA

The temporary nature of siRNA-induced gene silencing means that multiple doses of siRNA are required for a sustained therapeutic response. The Epps and Sullivan groups at the University of Delaware collaborated on a project with the Akins group at AI DuPont Nemours Hospital on using the photo-responsive polyplex system to improve healing in cardiac bypass graft junctions using the delivery of multiple siRNAs.<sup>30</sup> In this work, mPEG-*b*-P(APNBMA)<sub>n</sub> polyplexes were modified with Lipofectamine® and polyacrylic acid (PAA) to deliver siRNAs against an interleukin protein, IL1 $\beta$ , and a cadherin protein, CDH11, to human aortic adventitial fibroblasts (AoAFs). IL1 $\beta$  and CDH11 are involved in the over-proliferation of fibroblast cells at the bypass graft junction, which results in the weakening of the junction site.<sup>31</sup> Silencing the two proteins during bypass graft surgery was hypothesized to result in improved healing of the bypass graft junction. It was shown that the delivery of siRNA against IL1 $\beta$  and CDH11 halted the proliferation of AoAFs, which has clinical applications of reducing aortic bypass graft failures. Also, it was demonstrated that delivery of multiple doses of siRNA at controlled timepoints was necessary to sustain proliferation reduction. In a laboratory setting, multiple doses can be applied with repeated delivery of polyplexes. For clinical translation, it would be advantageous to deliver just one dose of polyplexes and use external stimuli to control delivery of multiple doses of siRNA.

Additionally, many medical applications involve silencing multiple genes of interest, thus requiring delivery of multiple siRNAs. For example, in many cancers, there are many dysregulated signaling pathways that are interdependent, and silencing multiple genes in a controlled fashion can result in a synergistic and favorable therapeutic response.<sup>32</sup> Delivering multiple siRNAs in one nanocarrier ensures equal cellular uptake of both siRNAs, which will enhance therapeutic success.<sup>32</sup>

#### **4.1.2 Research aim 3 - layered, photo-responsive nanocarriers for delivery of multiple siRNAs**

To co-deliver two different siRNAs in a single nanocarrier, the development of a layered, photo-responsive polyplex system was attempted in this work. The layered nanocarrier consisted of two layers of siRNAs and two layers of photo-responsive polymer. The work herein developed a successful method for producing layered nanocarriers. It was hypothesized that an initial UV stimulus would unpackage the outer layer of the polyplex to release the first layer of siRNA, and that a second UV stimulus would unpackage the inner layer of polymer and release the second layer of siRNA. The layered polyplex could be utilized in many applications that may benefit from sequential, controlled release of multiple doses of siRNA, such as the heart bypass graft work explored in the Epps and Sullivan groups.<sup>30</sup> With layered nanocarriers, it will ultimately be possible to use the photo-stimulus at different times to silence IL1 $\beta$  and CDH11 in a sustained fashion, which may further reduce the unwanted fibrotic response that weakens bypass graft junctions.

Figure 4-1 shows the design for the development of photo-responsive, layered nanocarriers. The outer layer of the polyplex consists of mPEG-*b*-P(APNBMA)<sub>7.9</sub>, which has been shown to release siRNA faster compared to the longer block co-

polymer.<sup>17,18</sup> In the initial design, the inner layer of polymer consisted of the longer diblock co-polymer, mPEG-*b*-P(APNBMA)<sub>23.6</sub>, which was chosen based on ease of availability of materials at the time. After an assessment of the initial design, a cationic homopolymer, P(APNBMA)<sub>29</sub>, was used as the inner layer of polymer to improve the layering process. The development and characterization the layered nanocarrier design formulations is described herein.

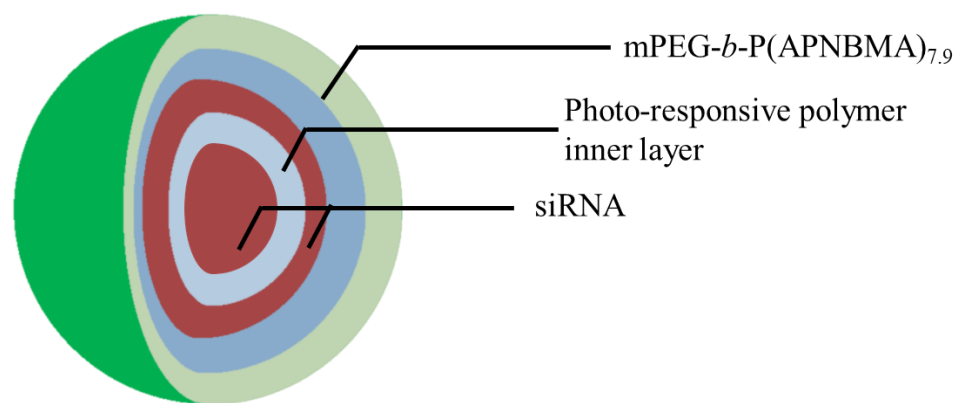


Figure 4-1. Schematic representation of the layered polyplex formulations explored in this work. Red indicates siRNA, blue indicates a photo-responsive polymer, and green indicates PEG block. The lighter blue photo-responsive polymer inner layer is varied in the experiments herein.

## 4.2 Results and discussion

### 4.2.1 Design 1 – Block copolymer inner layer

Based on ease of availability of materials, the initial formulation design used mPEG-*b*-P(APNBMA)<sub>7.9</sub> as the outer polymer layer and mPEG-*b*-P(APNBMA)<sub>23.6</sub> as the inner layer of polymer. The following sections discuss the challenges with the

initial design and suggestions for improvements in the next approach, Design 2, using a homopolymer inner layer.

#### 4.2.2 Simple formulation approach

The initial design entailed a simple formulation approach. Single-layer polyplexes were formulated with mPEG-*b*-P(APNBMA)<sub>23.6</sub> as described in Section 2.2.1, and scaled to 600  $\mu$ L of polyplexes with 4.8  $\mu$ g of siRNA in solution. Then, a second layer of 4.8  $\mu$ g of siRNA in 100  $\mu$ L of HEPES slowly was added to the mixture while gently vortexing over a period of 10 s. Nanocarriers were subsequently kept in a dark area for 20 min of incubation at 25 °C. Following incubation, 100  $\mu$ L of mPEG-*b*-P(APNBMA)<sub>7.9</sub> in HEPES slowly was added to the mixture while gently vortexing over a period of 10 s to form the outer layer of polymer at an N:P ratio of 4. Nanocarriers were subsequently kept in a dark area for another 20 min of incubation at 25 °C. In the initial procedure, there were no purification steps between adding each layer. Figure 4-2 shows a schematic representation of the initial proposed layering procedure.

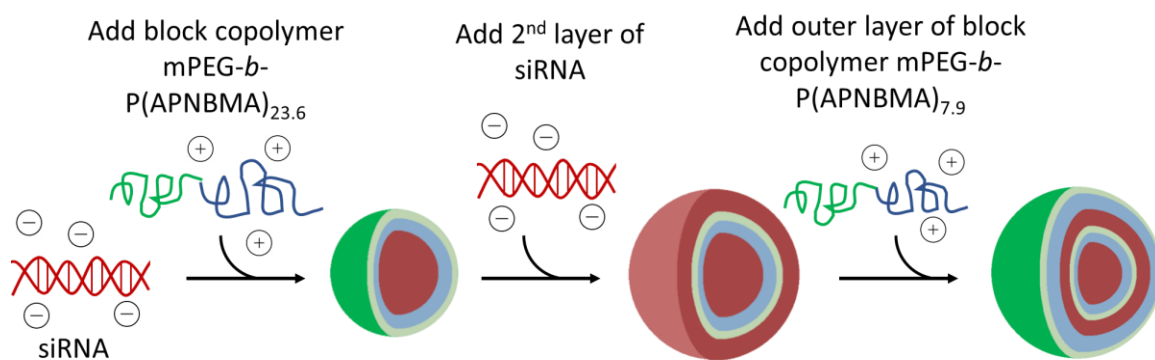


Figure 4-2. Proposed formulation of creating layered nanocarriers in Design 1 using block copolymers for each polymer layer.

If the layering experiment were to be successful, it would be expected that the zeta potential of the nanocarrier would be positive for the single-layer polyplex, negative when the second layer of siRNA was added, and positive again when the outer layer of polymer was added. Additionally, size may increase as each layer is added; however, there also is a possibility that particles may become more compact as additional charged components are added. Thus, size measurements alone cannot be used to determine successful layering and must be accompanied by measured changes in surface charge. Figure 4-3 shows the diameter size and zeta potential results for the initial layering experiment.

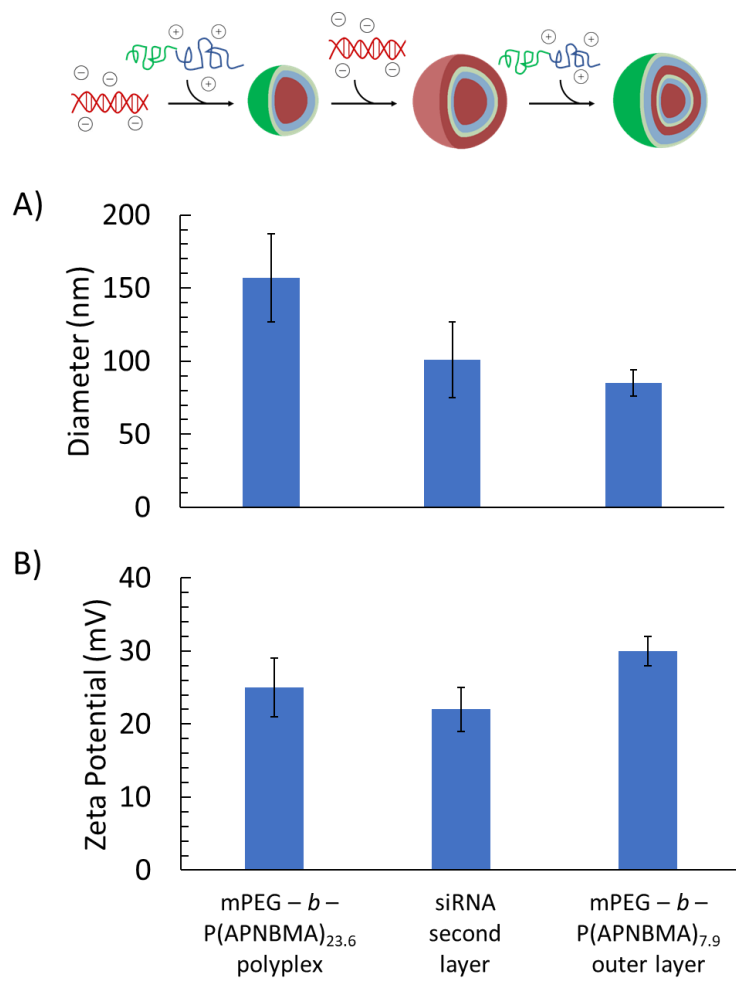


Figure 4-3. Initial proposed layering procedure using Design 1. A) Size measurements of nanocarriers. B) Zeta potential measurements of nanocarriers. Error bars indicate  $\pm 1$  standard deviation from 3 experimental replicates.

The zeta potential of the nanocarrier should be positive for the single-layer polyplex, negative when the second layer of siRNA is added, and positive again when the outer layer of polymer is added. The size and zeta potential trends did not follow

what would be expected for a successful layered polyplex design. Adding a second amount of siRNA and mPEG-*b*-P(APNBMA)<sub>7.9</sub> to the mPEG-*b*-P(APNBMA)<sub>23.6</sub> polyplexes resulted in a decrease in average size and had no statistically significant effect on the surface charge of the nanocarrier. During the formulation process, excess polymer and siRNA were not removed between each attempted layering step. It is hypothesized that instead of making any layered structures, the free polymer in solution leftover from making the single layer polyplex was complexing with siRNA from the second addition of siRNA to form more single-layer polyplexes. Adding the mPEG-*b*-P(APNBMA)<sub>7.9</sub> thus formed single layer mPEG-*b*-P(APNBMA)<sub>7.9</sub> polyplexes, which decreased the overall average size of the nanocarriers from 157 nm to 85 nm. The initial approach did not form layered polyplexes, and purification steps will be needed to layer the nanocarriers successfully.

#### **4.2.2.1 Revised formulation approach – centrifugation between layers**

One method of purifying nanocarriers between adding each layer is centrifugation. Deng et. al. successfully employed a simple centrifugation and resuspension strategy to purify siRNA-polycation layered nanoparticles between each layer addition.<sup>33</sup> It was hypothesized that centrifuging the polyplexes between each layer and resuspending the pellet would remove excess free polymer and siRNA in solution, thus allowing the layering process to occur. Figure 4-4 shows the results of the second formulation process for the initial nanocarrier materials design.

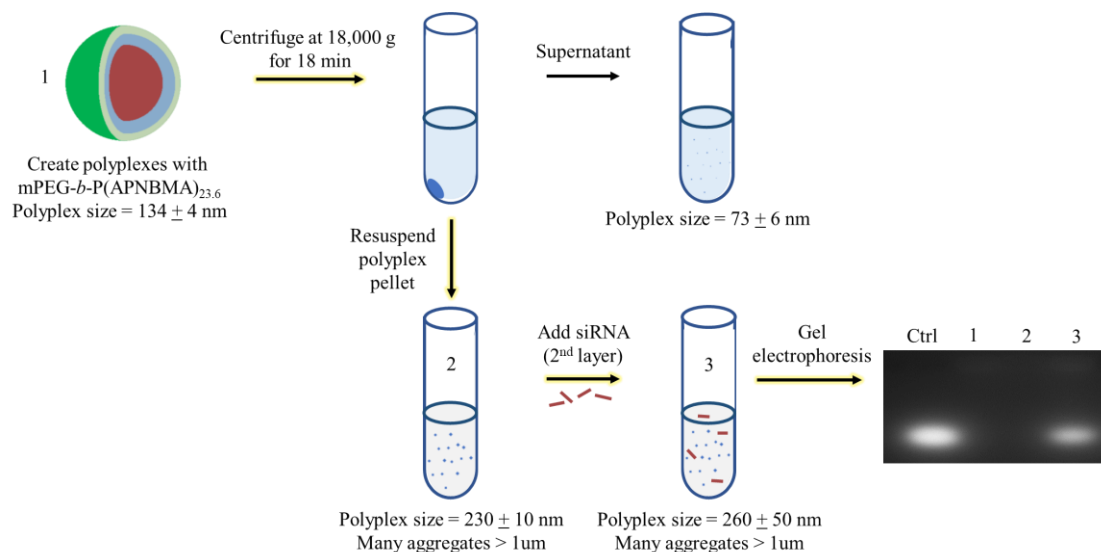


Figure 4-4. Procedural centrifugation purification steps for layered polyplex formulation using Design 1.

Polyplexes were created using mPEG-*b*-P(APNBMA)<sub>23.6</sub>, and size was measured with dynamic light scattering (DLS). The polyplexes had a diameter of ~130 nm, which is consistent with previous size measurements.<sup>17,18</sup> Sucrose was added at a 1 wt.% ratio to the polyplex solution in order to stabilize the solution and prevent aggregation during centrifugation. Polyplexes were centrifuged at 18,000 g for 18 min, based on procedures for similar types of polyplexes created by Deng, et.al.<sup>33</sup> The supernatant was collected, and the pellet was resuspended. The supernatant was analyzed *via* DLS, and it was found that there were particles with an average diameter of 73 nm in the supernatant. This suggests that the smaller polyplexes were not collected in the pellet and remained in the solution which contained excess free polymer. The resuspended pellet was analyzed *via* DLS. Particles in the purified solution had an average diameter of ~ 230 nm; however, there were also notable amounts of aggregates in solution with diameter greater than 1 μm.

A second aliquot of siRNA was added to the purified polyplexes. The average size of the polyplexes changed to ~ 260 nm upon the addition of the second aliquot, which is not different statistically from the size of the purified polyplexes alone. Furthermore, a gel electrophoresis assay showed that the second layer of siRNA did not stick to the polyplexes, as there was a significant amount of free siRNA in solution (band 3 in Figure 4-4). It is hypothesized that the PEG block on the polymer shielded the siRNA from being able to bind to the polyplex and create a layered structure. A potential solution is to use a homopolymer of P(APNBMA)<sub>n</sub> without the PEG block to formulate the inner polyplex structure for the layered nanocarrier, which is the revised design in Design 2.

#### **4.2.3 Design 2 – homopolymer inner layer**

To address concerns over the second layer of siRNA not being able to adhere to the PEG block, a homopolymer of P(APNBMA)<sub>29</sub> was synthesized by a post-doctoral research, Dr. Thu Vi, using modified synthesis steps from Green et.al.<sup>15</sup> A solution of 400  $\mu\text{L}$  of single-layer homopolymer polyplexes was created at an N:P = 4, with an siRNA concentration of 32  $\mu\text{g ml}^{-1}$  in 20 nM HEPES. For purification between adding each layer, the nanocarriers were centrifuged at 19,000 g for 20 min, which is a slight increase in both centrifuge speed and duration compared to the initial process. The intention of increasing the magnitude and length of the centrifugation was to recover more purified particles in the resuspended pellet. After resuspension, a solution of 100  $\mu\text{L}$  of HEPES containing 12.8  $\mu\text{g}$  of siRNA was added to form the outer layer of siRNA on the polyplex. After centrifugation and resuspension, the outer layer of mPEG-*b*-P(APNBMA)<sub>7,9</sub> in 100  $\mu\text{L}$  of HEPES was added at an N:P = 4 ratio relative to the second layer of siRNA. The revised formulation process for creating

layered nanocarriers with a homopolymer inner layer and purification steps between each layer addition is shown in Figure 4-5.

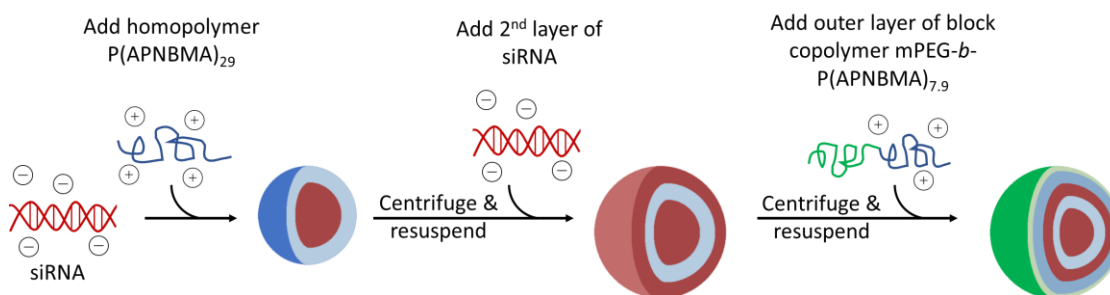


Figure 4-5. Revised layering formulation approach with homopolymer inner layer and purification *via* centrifugation between each layer addition.

During the revised layering process, the size and zeta potential of the nanocarriers were measured. As shown in Figure 4-6A, the size of the nanocarriers increased from ~ 125 nm to ~ 190 nm when adding a second layer of siRNA. There was no statistically significant increase in the nanocarrier size when adding the outer layer of mPEG-*b*-P(APNBMA)<sub>7,9</sub>. During the layering process, the surface charge of the single-layer homopolymer/siRNA nanocarriers was ~ 30 mV. With the addition of the second layer of siRNA, the zeta potential became negative at ~ -40 mV, which indicated successful incorporation of a second negatively charged siRNA layer. Furthermore, upon the addition of the outer layer of mPEG-*b*-P(APNBMA)<sub>7,9</sub>, the zeta potential became positive at ~ 25 mV, which suggests successful incorporation of the block copolymer outer layer. Zeta potential measurements are shown in Figure 4-6B.

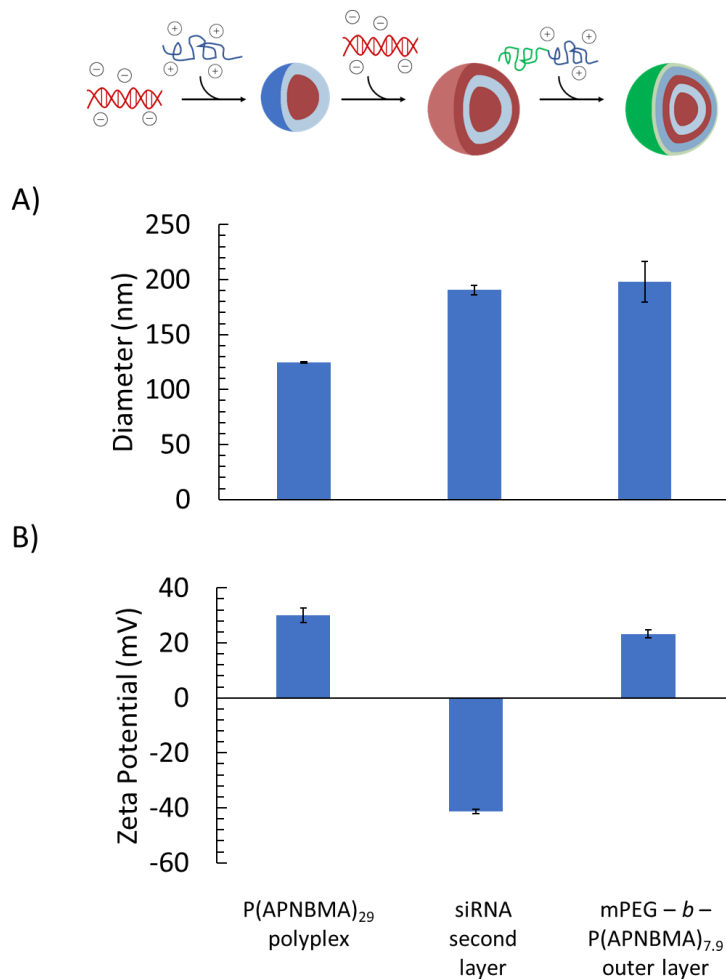


Figure 4-6. Revised layering procedure using Design 2 and homopolymer inner layer. A) Size measurements of nanocarriers. B) Zeta potential measurements of nanocarriers. Error bars indicate  $\pm 1$  standard deviation from 3 experimental replicates.

### 4.3 Conclusions

The work herein demonstrates that layered photo-responsive nanocarriers can be created for controlled delivery of multiple siRNAs from a single particle. A purification step was needed between adding each layer, and a cationic homopolymer had to be used to allow the second layer of siRNA to adhere.

In this work, we were able to develop a procedure for creating layered nanocarriers. Further experiments would be required to demonstrate successful controlled release of two distinct layers of siRNA. A plot of siRNA release over time for both the short block copolymer and the longer homopolymer would bring insight into the release characteristics of each polymer. Additionally, using gel electrophoresis after each layering step would provide information as to how much, if any, free siRNA exists in solution after adding each layer. Ultimately, independent control over the release of each layer of siRNA should be demonstrated. Figure 4-7 below shows an idea for demonstrating successful control over releasing each layer using hypothesized microscopy images. Cells would be transfected with DNA plasmids to express green and red fluorescent protein (GFP and RFP, respectively). GFP and RFP were chosen due to the commercial availability of siRNA to silence each protein. Layered polyplexes would be created with anti-GFP siRNA on the outside and anti-RFP siRNA on the inside. Over time, with increasing length of light exposure, GFP would be silenced first, followed by RFP.

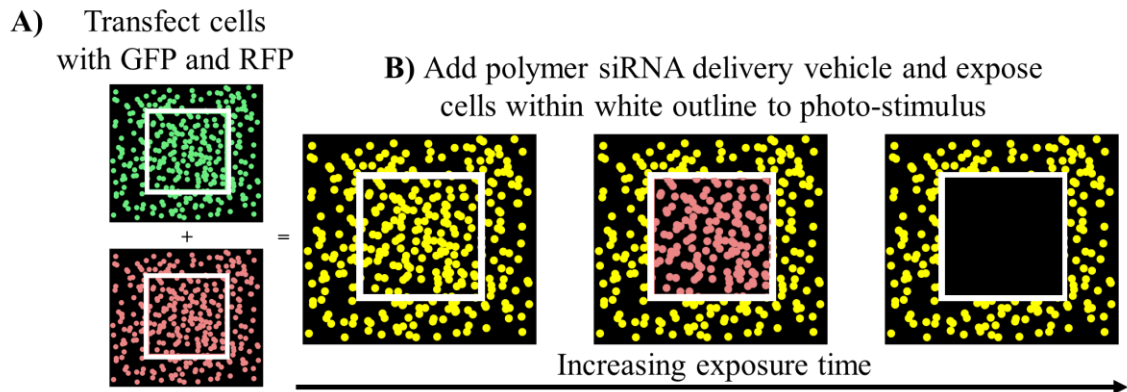


Figure 4-7. Representative microscopy images of proposed experiment to demonstrate successful control over releasing each layer of siRNA. A) Cells express both GFP and RFP. B) After delivering layered polyplexes, over increasing exposure to light stimulus, GFP will be silencing first, followed by RFP.

The layered system herein has many potential applications in medical treatments requiring repeated dosing of siRNA for sustained knockdown. Further research can also extend this layered system to deliver other components with siRNA, such as DNA, mRNA, or small molecule therapeutics.

## Chapter 5

### CONCLUSIONS

The field of polymer-based siRNA delivery has the potential to make advancements towards personalized medicine. The work herein addresses three research aims to improve the efficiency of siRNA delivery with photo-responsive polymer nanocarriers. The aims are as follows:

- 1) Optimize polyplex formulations by mixing two polymers of different lengths rather than synthesizing an entire polymer library
- 2) Incorporate kinetic modeling to optimize siRNA dosing schedules and improve research process efficiency
- 3) Deliver multiple siRNAs in a single polyplex by developing layered polymer nanocarriers

Towards Aim 1, it was demonstrated that mixing short and long strands of mPEG-*b*-P(APNBMA)<sub>n</sub> in siRNA polyplexes resulted in maximum amounts of gene silencing. Additionally, simple kinetic modeling was utilized to develop a dosing schedule for siRNA delivery to increase the research efficiency process, which addresses Aim 2. In looking at Aim 3, a procedure for developing layered photo-responsive nanocarriers for sequential delivery of two different siRNA was developed.

## Chapter 6

### FUTURE WORK

There are many possible paths for future with the photo-responsive siRNA delivery systems. Some possibilities include developing siRNA/small molecule co-delivery systems, creating thin film patches for siRNA delivery, and improving the photo-responsive polymer synthesis process.

#### 6.1 Co-delivery systems

The work herein aims to design a layered nanocarrier delivery system for a nanocarrier consisting of siRNA and photo-responsive polymer. The work could be further expanded to co-deliver an siRNA and a small molecule drug in a single layered nanocarrier. It has been suggested that combining gene and drug therapy techniques into a single nanomedicine can reduce cancer drug resistance.<sup>4,34</sup> For example, Ediriwickrema et. al. developed a layered polymer nanoparticle that contained an anticancer drug, camptothecin, and a plasmid encoding an apoptosis-inducing factor, which was shown to significantly reduce tumor growth compared to delivering the drug alone. One concern with chemotherapeutics is that they are highly toxic and there are a lot of off-target effect concerns. The spatiotemporal control that our system offers could help minimize off-target effects. For example, our research groups could use the layered nanocarrier approach to create a polyplex system with a small molecule drug like camptothecin at the core, followed by a layer of homopolymer, then a layer of siRNA, and coated in an outer layer of block copolymer. The layered nanocarrier system would provide independent controlled release of an siRNA and small molecule drug from the same particle. Exploring nucleic acid and

drug co-delivery with our photo-responsive polymer system would be a promising next-step of research.

## **6.2 Photo-responsive thin film for siRNA delivery**

There are many biomedical applications in which a polymer thin film method of therapeutic delivery is advantageous. Thin film delivery methods provide sustained treatment for localized health complications such as wound repair, and thin films also form a protective barrier around a site of injury to reduce infection and further re-opening of the wound.<sup>35</sup> For example, Castleberry, et. al., demonstrated that nylon thin film dressings coated with polyplex solutions provide improved methods for sustained localized siRNA delivery.<sup>36</sup> In another example, Flessner et. al. developed a layer-by-layer design of degradable polyelectrolyte-based films for the controlled release of siRNA from surfaces.

The photo-responsive polymer developed by the Epps and Sullivan labs could be utilized to develop photo-responsive thin films for siRNA delivery. Each application of light would stimulate the release of a specific layer of siRNA, and the film could be designed like the layered nanocarriers to provide controlled release of multiple siRNA cargo in a single film. A flow coating procedure could be used to coat alternating layered of photo-responsive polymer and siRNA onto a substrate. The film could then be transferred to a medical patch or bandage for localized application. Each film layer would be degraded by a different level of photo-stimulus, allowing for controlled release of each layer of siRNA.

## REFERENCES

1. Meister, G. & Tuschli, T. Mechanisms of gene silencing by double-stranded RNA. *Nature* **431**, 343–349 (2004).
2. Fire, A. *et al.* Potent and specific genetic interference by double-stranded RNA in *Caenorhabditis elegans*. *Nature* **391**, 806–811 (1998).
3. Whitehead, K. a, Langer, R. & Anderson, D. G. Knocking down barriers: advances in siRNA delivery. *Nat. Rev. Drug Discov.* **8**, 129–38 (2009).
4. Creixell, M. & Peppas, N. A. Co-delivery of siRNA and therapeutic agents using nanocarriers to overcome cancer resistance. *Nano Today* **7**, 367–379 (2012).
5. Oliveira, S., Storm, G. & Schiffelers, R. M. Targeted Delivery of siRNA. *J. Biomed. Biotechnol.* **2006**, 1–9 (2006).
6. Tomar, R. S., Matta, H. & Chaudhary, P. M. Use of adeno-associated viral vector for delivery of small interfering RNA. *Oncogene* **22**, 5712–5715 (2003).
7. Thomas, C. E., Ehrhardt, A. & Kay, M. a. Progress and problems with the use of viral vectors for gene therapy. *Nat. Rev. Genet.* **4**, 346–358 (2003).
8. Lehrman, S. Virus treatment questioned after gene therapy death. *Nature* **401**, 517–518 (1999).
9. Wang, J., Lu, Z., Wientjes, M. G. & Au, J. L.-S. Delivery of siRNA Therapeutics: Barriers and Carriers. *AAPS J.* **12**, 492–503 (2010).
10. Salzano, G., Costa, D. F., Torchilin, V. P. & Arabia, S. siRNA Delivery by Stimuli-Sensitive Nanocarriers. **21**, 4566–4573 (2016).
11. Cooper, B. M. & Putnam, D. Polymers for siRNA Delivery: A Critical Assessment of Current Technology Prospects for Clinical Application. *ACS Biomater. Sci. Eng.* **2**, 1837–1850 (2016).
12. Gary, D. J., Puri, N. & Won, Y. Y. Polymer-based siRNA delivery: Perspectives on the fundamental and phenomenological distinctions from polymer-based DNA delivery. *J. Control. Release* **121**, 64–73 (2007).
13. Johnson, R. N. *et al.* HPMA-oligolysine copolymers for gene delivery: Optimization of peptide length and polymer molecular weight. *J. Control. Release* **155**, 303–311 (2011).

14. Wang, Y. *et al.* Light-Responsive Nanoparticles for Highly Efficient Cytoplasmic Delivery of Anticancer Agents. *ACS Nano* **11**, 12134–12144 (2017).
15. Green, M. D. *et al.* Catch and release: photocleavable cationic diblock copolymers as a potential platform for nucleic acid delivery. *Polym. Chem.* **5**, DOI: 10.1039/C4PY00638K (2014).
16. Foster, A. A., Greco, C. T., Green, M. D., Epps, T. H. & Sullivan, M. O. Light-mediated activation of siRNA release in diblock copolymer assemblies for controlled gene silencing. *Adv. Healthc. Mater.* **4**, 760–770 (2015).
17. Greco, C. T., Epps, T. H. & Sullivan, M. O. Mechanistic Design of Polymer Nanocarriers to Spatiotemporally Control Gene Silencing. *ACS Biomater. Sci. Eng.* **2**, 1582–1594 (2016).
18. Greco, C. T., Muir, V. G., Epps, T. H. & Sullivan, M. O. Efficient tuning of siRNA dose response by combining mixed polymer nanocarriers with simple kinetic modeling. *Acta Biomater.* **50**, 407–416 (2017).
19. DANI, C. *et al.* Characterization of the transcription products of glyceraldehyde 3-phosphate-dehydrogenase gene in HeLa cells. *Eur. J. Biochem.* **145**, 299–304 (1984).
20. Bartlett, D. W. & Davis, M. E. Insights into the kinetics of siRNA-mediated gene silencing from live-cell and live-animal bioluminescent imaging. *Nucleic Acids Res.* **34**, 322–333 (2006).
21. Shen, W. *et al.* Screening of efficient polymers for siRNA delivery in a library of hydrophobically modified polyethyleneimines. *J. Mater. Chem. B* **4**, 6468–6474 (2016).
22. Wei, Z. *et al.* Paclitaxel-loaded Pluronic P123/F127 mixed polymeric micelles: Formulation, optimization and in vitro characterization. *Int. J. Pharm.* **376**, 176–185 (2009).
23. Miteva, M. *et al.* Tuning PEGylation of mixed micelles to overcome intracellular and systemic siRNA delivery barriers. *Biomaterials* **38**, 97–107 (2015).
24. Espié, P., Tytgat, D., Sargentini-Maier, M.-L., Poggesi, I. & Watelet, J.-B. Physiologically based pharmacokinetics (PBPK). *Drug Metab. Rev.* **41**, 391–407 (2009).

25. Varga, C. M., Hong, K. & Lauffenburger, D. A. Quantitative analysis of synthetic gene delivery vector design properties. *Mol. Ther.* **4**, 438–446 (2001).
26. Strand, S. P. *et al.* Molecular design of chitosan gene delivery systems with an optimized balance between polyplex stability and polyplex unpacking. *Biomaterials* **31**, 975–987 (2010).
27. Buyens, K. *et al.* Monitoring the disassembly of siRNA polyplexes in serum is crucial for predicting their biological efficacy. *J. Control. Release* **141**, 38–41 (2010).
28. Saltzman, W. M. & Olbricht, W. L. Building Drug Delivery Into Tissue Engineering. *Nat. Rev. Drug Discov.* **1**, 177–186 (2002).
29. M.A.C. Groenenboom, A.F.M. Maree, P. Hogeweg. The RNA silencing pathway: the bits and pieces that matter. *PLoS Comput. Biol.* **1**, 155–165 (2005).
30. Greco, C. T., Epps, III, T. H. & Sullivan, M. O. Attenuation of Maladaptive Responses in Aortic Adventitial Fibroblasts through Stimuli-Triggered siRNA Release from Lipid-Polymer Nanocomplexes. **1700099**, In Progress (2017).
31. Vamvakopoulos, J. E. *et al.* Interleukin 1 and chronic rejection: possible genetic links in human heart allografts. *Am. J. Transplant* **2**, 76–83 (2002).
32. Jang, M., Han, H. D. & Ahn, H. J. A RNA nanotechnology platform for a simultaneous two-in-one siRNA delivery and its application in synergistic RNAi therapy. *Sci. Rep.* **6**, 1–16 (2016).
33. Deng, Z. J. *et al.* Layer-by-layer nanoparticles for systemic codelivery of an anticancer drug and siRNA for potential triple-negative breast cancer treatment. *ACS Nano* **7**, 9571–9584 (2013).
34. Babu, A., Munshi, A. & Ramesh, R. Combinatorial therapeutic approaches with RNAi and anticancer drugs using nanodrug delivery systems. *Drug Dev. Ind. Pharm.* **43**, 1391–1401 (2017).
35. Mehrotra, S., Lee, I. & Chan, C. Multilayer mediated forward and patterned siRNA transfection using linear-PEI at extended N/P ratios. *Acta Biomater.* **5**, 1474–1488 (2009).

36. Castleberry, S., Wang, M. & Hammond, P. T. Nanolayered siRNA dressing for sustained localized knockdown. *ACS Nano* **7**, 5251–5261 (2013).

## Appendix

### TEXT AND FIGURE REPRINT PERMISSIONS

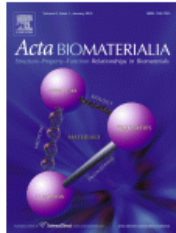


RightsLink®

Home

Create Account

Help



**Title:** Efficient tuning of siRNA dose response by combining mixed polymer nanocarriers with simple kinetic modeling

**Author:** Chad T. Greco,Victoria G. Muir,Thomas H. Epps,Millicent O. Sullivan

**Publication:** Acta Biomaterialia

**Publisher:** Elsevier

**Date:** 1 March 2017

© 2017 Acta Materialia Inc. Published by Elsevier Ltd. All rights reserved.

**LOGIN**

If you're a [copyright.com](#) user, you can login to RightsLink using your [copyright.com](#) credentials. Already a [RightsLink](#) user or want to [learn more?](#)

Please note that, as the author of this Elsevier article, you retain the right to include it in a thesis or dissertation, provided it is not published commercially. Permission is not required, but please ensure that you reference the journal as the original source. For more information on this and on your other retained rights, please visit: <https://www.elsevier.com/about/our-business/policies/copyright#Author-rights>

BACK

CLOSE WINDOW

Copyright © 2018 [Copyright Clearance Center, Inc.](#) All Rights Reserved. [Privacy statement](#). [Terms and Conditions](#).

Comments? We would like to hear from you. E-mail us at [customercare@copyright.com](mailto:customercare@copyright.com)